# Sustained exposure to the DNA demethylating agent; 2'-deoxy-5-azacytidine; leads to apoptotic cell death in chronic myeloid leukemia by promoting differentiation; senescence; and autophagy

Michael Schnekenburger, Cindy Grandjenette, Jenny Ghelfi, Tommy Karius, Bernard Foliguet, Mario Dicato, Marc Diederich


Title: Sustained exposure to the DNA demethylating agent; 2'-deoxy-5-azacytidine; leads to apoptotic cell death in chronic myeloid leukemia by promoting differentiation; senescence; and autophagy

Authors: Michael Schnekenburger, Cindy Grandjenette, Jenny Ghelfi, Tommy Karius, Bernard Foliguet, Mario Dicato, Marc Diederich

PII: S0006-2952(10)00792-6
DOI: doi:10.1016/j.bcp.2010.10.013
Reference: BCP 10745

To appear in: *BCP*

Received date: 12-8-2010
Revised date: 22-10-2010
Accepted date: 25-10-2010

Please cite this article as: Schnekenburger M, Grandjenette C, Ghelfi J, Karius T, Foliguet B, Dicato M, Diederich M, Sustained exposure to the DNA demethylating agent; 2'-deoxy-5-azacytidine; leads to apoptotic cell death in chronic myeloid leukemia by promoting differentiation; senescence; and autophagy, *Biochemical Pharmacology* (2010), doi:10.1016/j.bcp.2010.10.013

# Sustained exposure to the DNA demethylating agent, 2'-deoxy-5-azacytidine, leads to apoptotic cell death in chronic myeloid leukemia by promoting differentiation, senescence, and autophagy

Michael Schnekenburger [a], Cindy Grandjenette [a], Jenny Ghelfi [a], Tommy Karius [a], Bernard Foliguet [b], Mario Dicato [a], Marc Diederich [a, *]

[a] Laboratoire de Biologie Moléculaire et Cellulaire du Cancer, Hôpital Kirchberg, 9, rue Edward Steichen, L-2540 Luxembourg, Luxembourg.

[b] Laboratoire de microscopie électronique, Faculté de Médecine, 54500 Vandœuvre-lès-Nancy, France.

*: corresponding author: Tel: +352-2468-4040; Fax: +352-2468-4060; E-mail address: marc.diederich@lbmcc.lu; address: Laboratoire de Biologie Moléculaire et Cellulaire de Cancer, Hôpital Kirchberg, 9, rue Edward Steichen, L-2540 Luxembourg, Luxembourg.

**Abstract**

In addition to its demethylating properties, 5-aza-2'-deoxycytidine (DAC) induces cell cycle arrest, differentiation, cell sensitization to chemotherapy, and cell death. However, the mechanisms by which DAC induces antiproliferation via these processes and how they are interconnected remain unclear. In this study, we found that a clinically relevant concentration of DAC triggered erythroid and megakaryocytic differentiation in the human chronic myeloid leukemia (CML) K-562 and MEG-01 cell lines, respectively. In addition, cells showed a marked increase in cell size in both cell lines and a more adhesive cell profile for MEG-01. Furthermore, DAC treatment induced cellular senescence and autophagy as shown by β-galactosidase staining and by autophagosome formation, respectively. After prolonged DAC treatment, phosphatidyl serine exposure, nuclear morphology analysis, and caspase cleavage revealed an activation of mitochondrial-dependent apoptosis in CML cells. This activation was accompanied by a decrease of anti-apoptotic proteins and an increase of calpain activity. Finally, we showed that combinatory treatment of relatively resistant CML with DAC and either conventional apoptotic inducers or with an histone deacetylase inhibitor increased synergistically apoptosis. We therefore conclude that induction of differentiation, senescence, and autophagy in CML are a key in cell sensitization and DAC-induced apoptosis.

**Keywords:** 5-aza-2'-deoxycytidine, chronic myeloid leukemia, differentiation, senescence, autophagy, apoptosis.

## 1. Introduction

5-aza-2'-deoxycytidine (DAC) has been widely used as a DNA demethylating agent to reverse aberrant promoter hypermethylation that causes silencing of tumor suppressor genes (TSGs) believed to play a key role in carcinogenesis [1-3]. Although the antileukemic capacity of DAC has been widely documented, its therapeutic potential in hematologic malignancies is still under intensive investigation. Multiple clinical trials have shown the promising activity of low-dose DAC in leukemia, whereas its efficacy in solid tumors is rather limited [4-6]. Mechanisms underlying its anticancer activity are not fully understood, but it is believed to effectively suppress methylation-mediated gene silencing. The resulting DNA hypomethylation has been linked to its potent antiproliferative properties, where treatment causes a variety of outcomes. These effects include, for the most common, growth arrest, cell cycle perturbation, inhibition of DNA repair, upregulation of TSGs, inhibition of migration, invasion and metastasis, inhibition of angiogenesis, restoration of differentiation mechanisms, and induction of cell death [7-10]. The latter represent alternative cell fates, which under some circumstances are mutually exclusive [10]. Currently, factors that determine whether DNA methyltransferase (DNMT) inhibitors induce cell maturation versus apoptosis are unclear. In addition, although apoptosis has been considered as the typical mechanism for DAC-induced cell death, presently evidence is accumulating that alternative cell death pathways such as autophagy or senescence may play a role in tumor response to chemotherapy [11, 12]. These processes may therefore be considered within the context of classical chemotherapies to potentialize drug effects. Nevertheless, these mechanisms are largely undervalued concerning DAC treatments.

Chronic myeloid leukemia (CML) is an example of cancer where differentiation process is blocked in early steps of hematopoiesis and characterized by a multistep disease progression in which immature progenitor fails to give birth to cell lineage-restricted

phenotypes. Moreover, these cells acquire hyperproliferation capacity and apoptosis resistance [13]. One way cells bypass apoptotic pathway is by silencing several genes through DNA methylation. In this context, an attractive aspect is the ability of DAC to promote cyto-differentiation. Interestingly, DAC has shown an effect on differentiation *in vitro* and *in vivo* [9, 14-16]. However, the mechanisms of DAC-induced cell differentiation are not fully understood and especially their interconnections to apoptosis and alternative cell death pathways has not yet been investigated. We therefore wanted to better understand the biological response of leukemia with differentiation potential to clinically relevant dose of DAC. Thus, using human Bcr-Abl-positive CML cell models (K-562 and MEG-01 cells), we have identified multiple phenotypic changes after DAC exposure. These changes were associated to a removal of the differentiation block that characterizes CML. This response is also associated to an increase of specific markers of cellular senescence and autophagy. Moreover, prolonged DAC exposure triggered significant changes in gene expression network that control proliferation and apoptosis. Finally, we showed the combination of DAC with classical apoptotic inducers or with another epigenetic drug (*i.e.* HDAC inhibitor (HDACi)) increased synergistically apoptotic cell death in these cells. Together these findings revealed novel mechanisms underlying DAC-induced apoptotic cell death, which may account for sensitivity to other conventional drugs or HDACi and help to cope with the sensitivity/resistance to these drugs, in order to facilitate the design of future improved therapies in hematological malignancies.

## 2. Materials and methods

### 2.1. Cell culture and drug treatments

The human CML K-562 and MEG-01, and the human histiocytic lymphoma U-937 cell lines (Deutsche Sammlung für Mikroorganismen und Zellkulturen, Braunschweig, Germany), were

cultured in RPMI 1640 medium (Lonza, Verviers, Belgium) supplemented with 10% heat-inactivated fetal calf serum (Lonza) and 1% antibiotic–antimycotic (Lonza). Peripheral blood mononuclear cells (PBMCs) were purified from fresh buffy coats of four healthy adult human donors (Red cross, Luxembourg, Luxembourg) using the standard Ficoll-Hypaque (GE Healthcare, Roosendaal, The Netherlands) density separation method. All healthy volunteer donors gave informed consent. After three washes in Dulbecco's Phosphate Buffered Saline (DPBS, Lonza), cells were counted, and then resuspended in RPMI 1640 supplemented with with 10% heat-inactivated fetal calf serum and 1% antibiotic-antimycotic at a cell density of $2.10^6$ cells/ml. 5-aza-2'-Deoxycytidine (DAC), etoposide were purchased from Sigma-Aldrich (Bornem, Belgium), suberoylanilide hydroxamic acid (SAHA) from Cayman (Bio-connect, Huissen, The netherlands) and cisplatin from Teva pharmaceuticals (Platosin®, Bucharest, Romania).

**2.2. Assessment of cell viability and cell size**

After treatments, cells were processed through a semi-automated image-based cell analyzer (Cedex XS Innovatis, Roche, Luxembourg), which provides information about cell concentration and viability based on the Trypan Blue exclusion method.

**2.3. Methylation-sensitive restriction assay (MSRA)**

Genomic DNA was isolated using the DNeasy® Blood and Tissue Kit (Qiagen, Venlo, Netherlands) according to manufacturer's instructions and 1 µg was digested at 37°C by 20 U of the isoschizomer HpaII or MspI restriction endonucleases (New England Biolabs, Frankfurt am Main, Germany). After 16 h, 10 U of enzyme was added and incubated at 37°C for an additional 2 h. After incubation, the digestion mixture was resolved on 0.8% native agarose gel and the DNA was visualized by ethidium bromide staining.

### 2.4. Microscopic observations

Morphological changes were visualized using standard optics on a DMIRB inverted microscope equipped with a DFC350FX camera from Leica (Lecuit, Luxembourg, Luxembourg) and pictures were acquired using the Leica FireCam software. Pictures after benzidine and β-galactosidase staining were acquired using a Leica DM2000 equipped with a DFC420C and Leica FireCam software.

### 2.5. Assessment of differentiation

Erythroid differentiation was scored by the benzidine staining method as previously described [17]. Quantification of cell surface marker expression was performed by immunofluorescence staining. Briefly, $1.10^6$ cells were washed twice with 1X PBS, incubated 1 h at room temperature with fluorescein isothiocyanate (FITC)-conjugated antibodies against CD41 (BD Biosciences, Erembodegm, Belgium) and CD61 (DAKO, Heverlee, Belgium) or with primary anti-glycophorin A (GPA) antibody (Santa Cruz, Boechout, Belgium). GPA-labeled cells were then incubated 1 h at room temperature with a FITC-conjugated secondary antibody (Invitrogen, Tournai, Belgium). Isotype-matched immunoglobulins (BD Biosciences) were used as negative controls. Cells were washed and then analyzed by flow cytometry.

### 2.6. Platelet production analysis

Supernatants of DAC-treated MEG-01 cells were collected by centrifugation at 150 *g* for 10 min. Platelets were recovered from supernatants by sequential centrifugation (500 *g* for 10 min and 1 000 *g* for 10 min). Platelets were then labeled with an anti-CD61-FITC antibody and analyzed by flow cytometry. Platelets were identified based on their size (forward scatter characteristics (FSC)), the presence of CD61 expression, and lack of DNA as determined by

the absence of propidium iodide (PI, Sigma) staining using fresh human platelets as controls. Fresh human platelets had been obtained from Luxembourg Red Cross volunteer donors. All healthy volunteer donors gave informed consent.

### 2.7. RNA expression analysis by real-time PCR

Total RNA was extracted using NucleoSpin RNA II columns (Macherey-Nagel, Hoerdt France) according to the manufacturer's instructions. cDNA was synthesized by reverse transcription of 1 µg total RNA with SuperScript™ II RNase H$^-$ reverse transcriptase (Invitrogen) using oligo(dT) primers (Invitrogen). cDNAs were used as template for subsequent quantification by real-time PCR in a reaction mixture containing 1X Power SYBR® Green PCR Master Mix (Applied Biosystems, Halle, Belgium), and 0.1 µM of each primer (Table 1). Amplification was performed on an ABI 7300 real-time PCR system (Applied Biosystems) with an annealing-elongation step at 60°C for 60 s. Melting curve analyses were performed to ensure that a single product with the expected characteristics was obtained as preliminarily determined during primer tests. The amount of target gene was normalized to the endogenous level of β-actin using the $2^{-\Delta CT}$ method.

### 2.8. Flow cytometry acquisition and analysis

Flow cytometry acquisitions were performed on a FACSCalibur (BD Biosciences) using Cellquest software (BD Biosciences). Data were analyzed using either FlowJo software (Treestar, Ashland, OR, USA) or Win-MDI software (http://facs.scripps.edu/software.html).

### 2.9. Senescence-associated ß-galactosidase (SA-ß-gal) assay

SA-ß-gal activity was measured using the SA-ß-gal staining kit (Sigma) at pH 6 according to the manufacturer's instructions. Briefly, cells were washed twice with 1X PBS and fixed with

2% formaldehyde, 0.2% glutaraldehyde in 1X PBS for 6 min. Cells were then washed with 1X PBS and stained with a solution containing 5-bromo-4-chloro-3-indolyl-b-D-galactopyranoside (X-gal). Following overnight incubation at 37°C, cells were washed with 1X PBS and senescent cells were identified as blue-stained cells by standard light microscopy.

**2.10. Whole cell extracts and immunoblotting**

For preparation of whole cell extracts, $1.10^7$ cells were harvested, washed in cold 1X PBS, and lyzed in 1X Mammalian Protein Extraction Reagent (M-PER®, ThermoFisher, Erembodegem, Belgium) supplemented of 1X protease inhibitor cocktail (Complete®, Roche, Luxembourg, Luxembourg) according to the manufacturer's instructions. Protein concentration was measured using the Bradford assay. Proteins were aliquoted and stored at -80°C. Afterwards, proteins were subjected to sodium dodecyl sulfate (SDS)-polyacrylamide gel electrophoresis (PAGE) and transferred onto a Hybond™-P membrane (GE Healthcare, Diegem, Belgium). Membranes were pre-hybridized overnight at 4°C in 1X PBS containing 0.1% (v/v) Tween 20 (PBS-T) and 5% non-fat dry milk (NFDM). Blots were then probed in PBS-T containing the appropriate blocking agent (5% NFDM or 5% BSA) with the following primary antibodies: anti-beta-actin, anti-light chain 3 (LC3, Sigma), anti-BIM, anti-caspase-2, anti-caspase-3, anti-caspase-6, anti-caspase-7, anti-caspase-8, anti-caspase-9, anti-Bcl-xL (Santa Cruz), anti- B-cell lymphoma (Bcl)-2 (Calbiochem, Leuven, Belgium), anti- poly ADP ribose polymerase, (PARP), anti- X-linked inhibitor of apoptosis protein (XIAP, BD Biosciences), anti-Myeloid cell leukemia (Mcl)-1 (Cell Signaling, Leiden, The Netherlands), and anti-DNMT1 (Active motif, Rixensart, Belgium). After washing, blots were incubated with species-appropriate HRP-conjugated secondary antibody (Santa Cruz) in PBS-T containing 5% NFDM. Proteins of interest were detected with ECL Plus Western blotting

Detection System reagent (GE Healthcare) using a Kodak Image Station (Analis, Suarlée, Belgium).

**2.11. Transmission electron microscopy**

Cells were pelleted and fixed for 4 h in 2.5% glutaraldehyde (Euromedex, Mundolsheim, France) in 0.1 M sodium cacodylate buffer, pH 7.2 (Euromedex). Cells were then rinsed with sodium cacodylate buffer and postfixed in 1% osmium tetroxide (Euromedex) for 1 h at room temperature. Samples were washed and then dehydrated through a graded series of ethanol solutions to water followed by propylene oxide, and then infiltrated in 1:1 propylene oxide/poly Bed 812 (Euromedex). Samples were kept overnight embedded in Poly Bed 812, mounted in molds and left to polymerize in an oven at 56°C for 48h. Ultrathin sections (70-90 nm) were obtained with a Reichert-Jung Ultracut S microtome (Wien, Austria). Sections were stained with uranyl acetate and lead citrate, and subsequently examined with a CM12 transmission electron microscope (Philips, Eindhoven, The Netherlands).

**2.12. Evaluation of apoptosis by nuclear morphology and phosphatidyl exposure analyses**

Nuclear morphology was investigated by fluorescence microscopy using a cell^M imaging station from Olympus (Aartselaar, Belgium) on untreated and DAC-treated cells incubated 15 min at 37°C with the DNA-specific dye Hoechst 33342 (Sigma) and stained with PI. Quantification of the percentage of apoptotic cells was performed on the basis of their fragmented nuclei and the condensed chromatin beads around the periphery of the nucleus. Phosphatidyl serine exposure was assessed by flow cytometry using the AnnexinV–FITC Apoptosis Detection Kit I (BD Biosciences) following manufacturer's instructions.

### 2.13. Determination of calpain activity

Calpain activity was measured using Calpain Activity Assay Kit from Biovision (Gentaur, Kampenhout, Belgium) according to the manufacturer's instructions. Fluorescence was measured using a SpectraMax Gemini EM fluorometer from Molecular Probes (Invitrogen) and SoftmaxPro5 software.

### 2.14. Statistical analysis

Significant differences were determined using Student's *t*-test. Statistical significances were evaluated at $p<0.05$.

## 3. Results

### 3.1. DAC induces drastic morphological changes in CML K-562 and MEG-01 cells

We first examined the biological response of K-562 and MEG-01 cells to DAC exposure. Treatment with DAC did not result in any toxic effect on K-562 cells during the first 4 days of treatment (Figure lA). After 6 days of treatment, a modest increase of cell death was observed. Between 6 and 15 days, we observed a time-dependent increase of cell mortality reaching a maximum level of 95%. From a morphological point of view, the first noticeable effect of DAC on MEG-01 cells was a significant increase of adhering cells (Figure 1B and 1C). This was accompanied by an increase of cell sizes and changes in cell morphology. Then, the number of suspension cells was decreased concomitantly to an increase of cell death. Indeed, by the sixth day of culture, more than 60% of the treated cell showed a loss of cell viability leading to about 90% of cell death after 13 days of DAC exposure, while the number of adherent cells remained constant after 10 days of treatment. Under phase-contrast microscopy, adherent MEG-01 cells lost their round shape, developed pseudopoda extending from the cellular margins, and presented a cellular size up to 200 µM

(Figure 1B, see arrows). After 4 and 6 days of exposure, K-562 cell size (Figure 1B) increased with the appearance of vacuoles. Subsequently, number of these vacuoles decreased concomitant to an increase of their size between 6 and 13 days of treatment. These changes are accompanied by a time-dependent increase of cell death, reaching about 80% after 10 days. Additionally, microscopy observations revealed that continuous exposure led to a time-dependent increase of the diameter of some K-562 cells. To better characterize these progressive morphological changes, relative cell size and granularity of K-562 and MEG-01 cells were assessed by flow cytometry (Table 2). Cell size distribution curves were also analyzed on a Cedex XS counter (Table 2). Compared with untreated control cells, we observed a progressive increase in the granularity and the maximum peak diameters of viable cells in both CML cells.

Since DNMT1 catalyzes post-replicative DNA methylation and is responsible for maintaining the DNA methylation pattern during cell division, we determined the protein level of DNMT1 in K-562 and total MEG-01 cells before and after DAC treatment. Results show that both cell lines express comparable level of DNMT1 protein (Figure 2A). To determine whether DAC-induced morphological changes could be due to the demethylating properties of this compound ,we investigated the level of genomic DNA methylation by MSRA. Figure 2B shows a time-dependent genomic DNA demethylation following DAC exposure in both CML cell lines.

### 3.2. DAC treatment induces erythroid differentiation of K-562 cells and megakaryocytic differentiation of MEG-01 cells

K-562 can be differentiated into various lineages depending of the inducer and MEG-01 can be differentiated toward the megakaryocytic pathway with several agents [18, 19]. Based on our previous observations (Figure 1 and Table 2), and red pellets observed in K-562 cells (Figure 3A, upper panel) after DAC exposure, we decided to investigate whether DAC

can induce cyto-differentiation in our cell models. Benzidine-positive cells (blue staining in Figure 3A, lower panel) corresponding to hemoglobin synthesis increased in K-562 cells in a time-dependent manner and reached 55% after 6 days of treatment (Figure 3A, lower panel). After 6 days, the number of hemoglobin-positive cells remained essentially constant (data not shown). In contrast, DAC did not induce MEG-01 benzidine-positive cells (data not shown). To further characterize the ability of DAC to induce differentiation in K-562 and MEG-01 cells, we investigated CD41 and CD61 expression as specific markers for megakaryocytic differentiation as well as GPA expression as a specific marker for erythroid differentiation. As shown in Figure 3B, although untreated K-562 cells are already expressing GPA, DAC treatment led to a significant increase of this marker after 4 days. In addition, CD41 and CD61 expression remained unaffected by DAC exposure. In contrast, in MEG-01 cells, which are positive for GPA expression, DAC induced a significant decrease of GPA expression. However, DAC-treated MEG-01 cells became positive to CD41 and CD61 expression. Furthermore, kinetic analysis demonstrated a time-dependent induction of erythroid and megakaryocytic markers in K-562 and MEG-01, respectively (Figure 3C). We did not detect any significant change in CD11b, CD14 and CD45 expression as markers of myeloid, monocytic and leucocytic differentiation, respectively (data not shown). These results demonstrated that DAC induced only erythroid differentiation in K-562 based on the increase of GPA expression, the production of hemoglobin, and the absence of megakaryocytic markers. Finally, we completed this study by analyzing the particles derived from MEG-01, as this cell line is able to produce platelets similar in structure to freshly isolated human platelets [18]. DAC treatment of MEG-01 cells for 4 days caused an increase in platelets production (Figure 3D, upper panel). These particles are similar in size (forward scatter) and granularity (side scatter) to normal human platelets. In addition, platelets derived from MEG-01 cells express the platelet marker CD61 (Figure 3D, lower panel), and they lack

DNA as determined by the absence of propidium iodide staining (data not shown). These data indicate that MEG-01-derived particles are similar to normal human platelets and that DAC triggered megakaryocytic differentiation of MEG-01 cells.

To determine whether DAC had an extensive effect on erythroid- and megakaryocytic-specific genes, we analyzed the expression of various genes implicated in differentiation processes. Results showed a general positive effect on erythroid-specific genes expression in DAC-mediated erythroid differentiation of K-562 cells (Figure 3E). Indeed, mRNAs of genes involved in hemoglobin synthesis namely *α-globin* and *γ-globin* were up-regulated in a time-dependent manner following DAC treatment. *β-globin* mRNA expression remained unaffected by DAC treatment. The transcription factor *MafK* was also induced in a time-dependent manner. On the other hand, the erythropoietin receptor (*EpoR*) as well as erythroid-specific transcription factors *GATA1* and Nuclear factor-erythroid 2 (*NF-E2*) *p45* were transiently increased with a maximum after 4 days of treatment, whereas *GATA2* was presenting a tendency to decrease. In MEG-01 cells (Figure 3F), *GATA2* mRNA expression was increase in a time-dependent manner, whereas *GATA1* expression was transiently decreased. *NF-E2p45* expression remained stable during the time of DAC treatment. Interestingly, E-Cadherin (*CDH1*) and *MafK* mRNAs were up-regulated in a time-dependent manner.

### 3.3. DAC induces senescence and autophagy

Increase of vacuole number and cell size for both cell lines (Figure 1B) prompted us to evaluate whether cellular senescence and autophagy processes could be triggered by DAC treatment. To investigate the impact of DAC on cellular senescence, SA-β-Gal activity was assessed. K-562 cells treated with doxorubicin for 4 days were used as positive control of senescence induction. K-562 and both adherent and suspension MEG-01 cells stained

positively for β-galactosidase (Figure 4A, blue stain). K-562 and MEG-01 cells showed a high proportion of senescent cells compared to untreated cells (Figure 4B).

Both cell lines were further investigated for autophagy by following microtubule-associated protein light chain 3 (LC3) conversion of LC3-I to LC3-II, which is widely used to monitor autophagy by its localization to the autophagosomal membranes [20]. DAC treatment induced a robust conversion from LC3-I to LC3-II in DAC treated K-562 and both MEG-01 populations (Figure 4C). To confirm the conversion of LC3, we monitored autophagosomal structure formation by electron microscopy. As shown in Figure 4D, autophagic vacuoles surrounded by a double-layered membrane and containing cytoplasmic constituents were observed in DAC-treated CML cells.

### 3.4. DAC-induced cell death in CML cells is mediated by the intrinsic pathway of apoptosis

Then, we analyzed the induction of apoptosis in DAC-treated CML cells. Apoptosis was firstly evaluated by nuclear morphological changes in DAC-treated leukemia cells. Conversely to cell viability (Figure 1A), K-562 and MEG-01 cells showed distinct morphological features of apoptosis in a time-dependent manner (Figure 5A). In K-562 cells, the percentage of apoptotic cells was modest (14%) after 6 days of treatment but slowly and continuously increased (to greater than 85%) with DAC exposure times up to 13 days (Figure 5B). Similarly, MEG-01 cells exposed to DAC became weakly apoptotic (18%) after 3 days of treatment and continuously increased (to greater than 85%) with DAC exposure times up to 10 days. In contrast, no significant apoptosis was induced in adherent MEG-01 population. Apoptosis was confirmed by the continuous increase of phosphatidyl serine externalization as represented by annexin-FITC/PI double staining of DAC-treated K-562 and MEG-01 cells (Figure 5C).

Since caspases play a crucial role in the mediation of apoptosis, we investigated the activation of caspases specificically involved in different apoptotic pathways (Figure 5D). DAC treatment induced the initiator pro-caspase 9 cleavage as well as the cleavage of poly-ADP-ribose polymerase (PARP), without activation of the initiator pro-caspase 8 in K-562 and suspension MEG-01 cells, suggesting that the receptor-mediated apoptotic pathway is not implicated. Furthermore, a weak pro-caspases 3 and 2 processing was observed in suspension MEG-01 cells. In contrast, effector pro-caspases 2, 6, and 3 were not activated in K-562 cells. Strikingly, the profile of caspase 7 activation following DAC exposure showed an interesting pattern. Indeed, in control MEG-01 cells as well as in total population at day 1 and 2 of DAC treatment, both 34-and 30-kDa forms were observed as in U-937 control. After 3 days of treatment, only 34-/30-kDa forms were observed in suspension and adherent MEG-01 cells, respectively. In contrast, in K-562 cells, the 20-kDa form appeared only at late time of treatment.

Since pro- and anti-apoptotic proteins control apoptotic pathways, we therefore analyzed the expression of several of these proteins (Figure 5E). DAC down-regulated the anti-apoptotic proteins Bcl-2 and XIAP in K-562 and suspension MEG-01 cells. Interestingly, the decrease of Bcl-2 was observed after a transient increase in both CML cells. The anti-apoptotic protein Mcl-1 was decreased in MEG-01 and remained unaffected in K-562 cells. Strikingly, the pro-apoptotic protein Bcl-xL was up-regulated in K-562, whereas it was down-regulated in MEG-01 cells.

### 3.5. DAC-induced apoptosis is accompanied by an increase of calpain activity

The pattern of caspase activation observed after DAC treatment prompted us to determine if alternative pathways could mediate DAC-induced apoptosis. Considering the role of calpain in apoptosis [21], we investigated calpain activity after DAC exposure. DAC

induced a time-dependent increase of calpain activity in K-562 cells. Interestingly, in MEG-01 cells, we observed only a moderated but significant increase of calpain activity in the suspension population, whereas this activity was decreased in adherent MEG-01 cells (Figure 6).

**3.6. DAC in combination to conventional or epigenetic drugs have synergistic effects on the survival of CML cells**

Finally, we wanted to evaluate whether the typical resistance to apoptosis that characterized CML cells, conferred by the chimaeric non-receptor tyrosine kinase p210 Bcr-Abl, was weakened by DAC-induced differentiation. First, we used cisplatin and etoposide as known apoptogenic inducers, which alone had only a modest effect on cell death in K-562 and MEG-01 cell lines (Figure 7A). After a 3-day pretreatment with DAC, cisplatin or etoposide treatments synergistically induced apoptotic cell death in comparison to the modest effect produced by either agent alone.

Similarly, binary treatment with the HDACi, SAHA, and DAC synergistically induced apoptosis compared to the treatment with either agent alone (Figure 7B). Interestingly, among the various conditions tested, the most successful conditions were to treat cells with DAC for 5 days prior a treatment for 2 days with SAHA. Indeed, the rate of apoptosis was increase from 13% and 17% after SAHA and DAC, respectively, to 57% when used in combination.

Finally, we investigated the effect of these treatments on cell viability of PBMCs from healthy donors. Figure 7C indicates that none of the treatments used alone or in combination exert a significant effect on cell viability of PBMCs.

## 4. Discussion

Epigenetic alteration such as DNA methylation-dependent gene silencing of TSGs is frequently found in human cancers and has led to the development of epigenetic drugs such as the DNA demethylating agent DAC, which targets a fundamental mechanism of transcriptional control. It has been shown that DAC has potent antitumor activity, especially in hematological malignancies. Depending on the cell type, this activity could be related to cell cycle perturbation, inhibition of DNA repair, upregulation of TSGs, inhibition of migration, invasion and metastasis, inhibition of angiogenesis, restoration of differentiation mechanisms, and/or induction of cell death. In addition, these processes could be methylation-dependent or methylation-independent [4, 5, 7-10]. Although, a large amount of literature is describing this various aspects, few reports have investigated the effect of prolonged DAC exposure inducing cell differentiation and leading to cell death. The results presented herein demonstrated that upon clinically relevant dose of DAC [22], CML cells showed a propensity to differentiate and to induce autophagy as well as senescence, which could explain cell sensitization to other therapeutic drugs. Nevertheless, under sustained DAC exposure, cells subsequently triggered intrinsic apoptotic cell death, which was accompanied of an increase of calpain activity.

The cell line MEG-01 has been shown to undergo megakaryocytic differentiation by the mean of megakaryocyte maturation and platelet production [18]. Our results demonstrated that MEG-01 cells treated with DAC exhibited features of cells committed to megakaryocytic differentiation as shown by: (i) the lost of their round shape concomitant to the increase of cellular adherence and the appearance of long cytoplasmic protrusions; (ii) an increase of megakaryocytic surface markers concomitantly to a decrease of the erythroid marker GPA; and (iii) the production of particles with similar characteristics of freshly isolated human platelets. These results are in accordance to mature megakaryocytes, which

are the direct platelet precursors, able to produce platelets arising from the development of these long and thin cytoplasmic extensions seen in morphological analyses and called proplatelets. Proplatelet formation requires profound changes in the organization of the cytoskeleton, which are regulated by several transcription factors required for the megakaryocytic differentiation program. These transcription factors are including GATA1, GATA2, and NF-E2 [23]. Indeed, upon DAC exposure, we observed an increase of *GATA2* and *NF-E2* expression and a transient decrease of *GATA1* expression. This particular profile of expression could be explained by the fact that both GATA1 and GATA2 are required for megakaryocytic differentiation. Indeed, it has been shown that GATA2 promotes megakaryocytic commitment, whereas GATA1 is involved in megakaryocytic maturation [24-26]. In addition, it has been shown that NF-E2 expression is increased in $CD34^+$ cells during thrombopoietin-induced megakaryocytic differentiation [27]. Accordingly to the increase of cellular adherence and differentiation, detected in DAC-treated MEG-01 cells, we also measured an increase of *CDH1* mRNA expression. Indeed, E-cadherin mediates cell contacts and acts as an important suppressor of epithelial tumor cell invasiveness and metastasis. In addition, defects in its expression or function have been associated with poorly differentiated cells and tumor progression, and therefore E-cadherin is considered as a TSG [28]. Since it was reported that methylation of the E-cadherin promoter in cancer cells may reduce its gene expression [29], perhaps E-cadherin promoter is methylated in MEG-01 cells. Thus, DAC-enhanced E-cadherin gene expression might be mediated through DNA demethylation. However, additional experiments will be required to confirm this hypothesis. Taken together, these results suggested that the transcriptional changes of those various genes might contribute to DAC-induced differentiation, and therefore enhancing platelet production may provide therapeutic benefit in the treatment of thrombocytopenia.

DAC-induced megakaryocytic differentiation was associated to cellular senescence and caused a slow induction of apoptosis. Interestingly, cells presenting enlarged cell morphology coincide with cells presenting the strongest acidic SA-ß-gal activity, which is characteristic of senescent cells. Mitochondria-dependent apoptotic cell death is associated to caspase 9 cleavage/activation, caspase-3 mild induction and PARP cleavage. These results were consistent with platelet formation, where senescent megakaryocytes undergo apoptosis as the consequence of a caspase-dependent mechanism after platelet release [30].

The cell line K-562 can be differentiated into various lineages depending of the inducer and has been widely used as a model for leukemia differentiation [19]. Our data revealed that DAC induced a significant number of K-562 cells exhibiting erythroid-like features, such as an induction of both GPA and *EpoR* expression, and hemoglobin-producing cells. In the literature, hemoglobin production has been reported in K-562 after DAC treatment [16]. Furthermore, we demonstrated that DAC induced the expression of several genes involved in erythroid maturation. Indeed, we showed that mRNA expression of specific transcription factors involved in erythropoiesis regulation such as *NF-E2* and *GATA1* were increased in DAC-treated cells in correlation with hemoglobin production concomitantly to erythroid differentiation. NF-E2 is required for generating normal erythrocytes in mice given that its absence results in red blood cell abnormalities, including hypochromia, anisocytosis and reticulocytosis [31]. The increase in *NF-E2p45* subunit was in agreement with *α*- and *γ-globin* over-expression after DAC exposure since this transcription factor is involved in the transcription regulation of these genes. The transcription factors GATA1 and GATA2 specifically bind to this genes in a competitive manner. GATA1 was widely described as required for erythroid maturation whereas GATA2, which is involved at the beginning of erythropoiesis, rapidly participates to megakaryocytic pathway commitment if its expression level is sustained [32]. In this context, *GATA2* showed a tendency to decrease

in agreement to *GATA1* up-regulation after DAC-induced erythroid differentiation. Interestingly, these results are sustained by previous report showing DAC is able to stimulate hemoglobin production in patients with sickle cell disease [33].

Similarly to our observations with MEG-01 cells, DAC-mediated erythroid differentiation in K-562 cells caused a slow activation of caspases followed by apoptosis. Caspase activation is required for terminal erythroid differentiation [34]. This induction is associated to a modulation of the expression of anti- and pro-apoptotic Bcl-2 family members. Strikingly, we detected an increased Bcl-2 and Bcl-xL expression, followed by a down-regulation at late stage of differentiation concomitantly to apoptosis induction in DAC-treated K-562 cells. Conversely, it has been demonstrated that, on one hand, these factors are induced to presumably protect erythroblasts from apoptosis and, on the other hand, that prolonged erythroid differentiation in K-562 cells leads to a downregulation of these factors [35, 36].

Although the activation of caspase 9 and 7 associated to PARP cleavage strongly suggests that DAC induced a mitochondrial-dependent apoptosis in K-562 cells, we did not detect the cleavage of caspase 2, 6 or 3. The latter caspase is responsible for caspase 7 activation. However, in agreement with our results, calpains could be implicated in DAC-mediated apoptosis. Indeed, several calpains are frequently activated in apoptosis and involve elevated intracellular calcium concentration [21]. In addition, it has been recently reported that calpain 1 could also activate caspase 7 [37]. In addition, a large amount of evidence is showing that calpains mediate the proteolytic cleavage of substrates specifically involved in various cellular processes during differentiation and cell death. Thus, calpains are also involved in senescence [38]. Furthermore, calpains positively modulate autophagy to limit the accumulation of damaged organelles and proteins, and then cleave essential autophagic

proteins, such as ATG5 leading to an apoptotic switch [39]. A recent report showed that autophagy is required for senescence transition in mammalian cells [40].

To our knowledge, it is the first report showing that autophagy might be involved in DAC-induced cytotoxicity in human CMLs. Although the identification of autophagy was unexpected, the formation of autophagasomes was clearly shown by LC3-I to LC3-II conversion, indicating that DAC enhanced formation of autophagosomes, which was further demonstrated by electron microscopy analysis. Conversely, it remains to study if autophagy is either related to the induction of survival mechanisms or mediates apoptotic cell death.

Although further studies are required to dissect the mechanism and the connection between differentiation, autophagy, senescence and apoptosis during DAC-induced cell death and the relevance of calpains in these processes, the time course of events provides additional evidence that differentiation, autophagy, and senescence precede the manifestation of apoptosis. Thus, it would be worthwhile to investigate whether the induction of senescence and autophagy are related to epigenetic mechanisms and are therefore a consequence of DNA methylation, and/or whether these mechanisms are compound-specific. These aspects are under current investigation in our laboratory.

While short-time DAC exposure did not kill resistant CML cells, it can sensitize cells to apoptosis induced by either conventional drugs or HDACi. Regarding the temporal order of events, this sensitization could be based on DAC-induced senescence and autophagy mechanisms. Indeed, cellular senescence impairs the replication potential of a cell, thus preventing cell proliferation in the various stages of neoplastic progression. Autophagy is a lysosomal degradation pathway essential for homeostasis, which can be initially regarded as a survival mechanism, however it may reportedly contribute to cell death by its self-digesting system [11, 12]. Therefore, in order to improve leukemia therapies, senescence induced-

therapy using DAC should be considered in combination with classic apoptotic inducing chemotherapeutic strategies and/or associated to a modulation of the autophagic process.

In conclusion, this study has identified that DAC-induced cell death is mediated through the activation of differentiation, autophagy, and senescence, which lies upstream of subsequent apoptotic cell death. Understanding how these alternative cell death pathways intertwined and can be modulated represents now a major challenge for future improving efficacy of current chemotherapies with epigenetic drugs in the treatment of hematological malignancies.

**Acknowledgements**

This work was supported by the “Recherche Cancer et Sang” foundation, the “Recherches Scientifiques Luxembourg” association, by the “Een Häerz firkriibskrank Kanner” association, by the Action Lions “Vaincre le Cancer” association and by Télévie Luxembourg. MS and JG are recipients of a Télévie Luxembourg fellowship. CG and TK are supported by AFR fellowships from the National Research Fund, Luxembourg. Publication costs are covered by the Fonds National de la Recherche Luxembourg.

**References**

[1] Esteller M. Aberrant DNA methylation as a cancer-inducing mechanism. Annu Rev Pharmacol Toxicol 2005;45:629-56.

[2] Lyko F, Brown R. DNA methyltransferase inhibitors and the development of epigenetic cancer therapies. J Natl Cancer Inst 2005;97:1498-506.

[3] Stresemann C, Lyko F. Modes of action of the DNA methyltransferase inhibitors azacytidine and decitabine. Int J Cancer 2008;123:8-13.

[4] Issa JP, Garcia-Manero G, Giles FJ, Mannari R, Thomas D, Faderl S, et al. Phase 1 study of low-dose prolonged exposure schedules of the hypomethylating agent 5-aza-2'-deoxycytidine (decitabine) in hematopoietic malignancies. Blood 2004;103:1635-40.

[5] Kantarjian HM, O'Brien S, Cortes J, Giles FJ, Faderl S, Issa JP, et al. Results of decitabine (5-aza-2'deoxycytidine) therapy in 130 patients with chronic myelogenous leukemia. Cancer 2003;98:522-8.

[6] Schmelz K, Sattler N, Wagner M, Lubbert M, Dorken B, Tamm I. Induction of gene expression by 5-Aza-2'-deoxycytidine in acute myeloid leukemia (AML) and myelodysplastic syndrome (MDS) but not epithelial cells by DNA-methylation-dependent and -independent mechanisms. Leukemia 2005;19:103-11.

[7] Miller-Kasprzak E, Jagodzinski PP. 5-Aza-2'-deoxycytidine increases the expression of anti-angiogenic vascular endothelial growth factor 189b variant in human lung microvascular endothelial cells. Biomed Pharmacother 2008;62:158-63.

[8] Nam JS, Ino Y, Kanai Y, Sakamoto M, Hirohashi S. 5-aza-2'-deoxycytidine restores the E-cadherin system in E-cadherin-silenced cancer cells and reduces cancer metastasis. Clin Exp Metastasis 2004;21:49-56.

[9] Pinto A, Attadia V, Fusco A, Ferrara F, Spada OA, Di Fiore PP. 5-Aza-2'-deoxycytidine induces terminal differentiation of leukemic blasts from patients with acute myeloid leukemias. Blood 1984;64:922-9.

[10] Selvakumaran M, Reed JC, Liebermann D, Hoffman B. Progression of the myeloid differentiation program is dominant to transforming growth factor-beta 1-induced apoptosis in M1 myeloid leukemic cells. Blood 1994;84:1036-42.

[11] de Bruin EC, Medema JP. Apoptosis and non-apoptotic deaths in cancer development and treatment response. Cancer Treat Rev 2008;34:737-49.

[12] Vicencio JM, Galluzzi L, Tajeddine N, Ortiz C, Criollo A, Tasdemir E, et al. Senescence, apoptosis or autophagy? When a damaged cell must decide its path--a mini-review. Gerontology 2008;54:92-9.

[13] Melo JV, Barnes DJ. Chronic myeloid leukaemia as a model of disease evolution in human cancer. Nat Rev Cancer 2007;7:441-53.

[14] Creusot F, Acs G, Christman JK. Inhibition of DNA methyltransferase and induction of Friend erythroleukemia cell differentiation by 5-azacytidine and 5-aza-2'-deoxycytidine. J Biol Chem 1982;257:2041-8.

[15] Attadia V. Effects of 5-aza-2'-deoxycytidine on differentiation and oncogene expression in the human monoblastic leukemia cell line U-937. Leukemia 1993;7 Suppl 1:9-16.

[16] Fabianowska-Majewska K, Wyczechowska D, Czyz M. Inhibition of dna methylation by 5-aza-2'-deoxycytidine correlates with induction of K562 cells differentiation. Adv Exp Med Biol 2000;486:343-7.

[17] Schnekenburger M, Morceau F, Duvoix A, Delhalle S, Trentesaux C, Dicato M, et al. Increased glutathione S-transferase P1-1 expression by mRNA stabilization in hemin-induced differentiation of K562 cells. Biochem Pharmacol 2004;68:1269-77.

[18] O'Brien JJ, Spinelli SL, Tober J, Blumberg N, Francis CW, Taubman MB, et al. 15-deoxy-delta12,14-PGJ2 enhances platelet production from megakaryocytes. Blood 2008;112:4051-60.

[19] Tsiftsoglou AS, Pappas IS, Vizirianakis IS. Mechanisms involved in the induced differentiation of leukemia cells. Pharmacol Ther 2003;100:257-90.

[20] Mizushima N, Yoshimori T. How to interpret LC3 immunoblotting. Autophagy 2007;3:542-5.

[21] Kar P, Samanta K, Shaikh S, Chowdhury A, Chakraborti T, Chakraborti S. Mitochondrial calpain system: an overview. Arch Biochem Biophys 2010;495:1-7.

[22] Aparicio A, Eads CA, Leong LA, Laird PW, Newman EM, Synold TW, et al. Phase I trial of continuous infusion 5-aza-2'-deoxycytidine. Cancer Chemother Pharmacol 2003;51:231-9.

[23] Kaushansky K. Historical review: megakaryopoiesis and thrombopoiesis. Blood 2008;111:981-6.

[24] Visvader JE, Elefanty AG, Strasser A, Adams JM. GATA-1 but not SCL induces megakaryocytic differentiation in an early myeloid line. EMBO J 1992;11:4557-64.

[25] Ikonomi P, Rivera CE, Riordan M, Washington G, Schechter AN, Noguchi CT. Overexpression of GATA-2 inhibits erythroid and promotes megakaryocyte differentiation. Exp Hematol 2000;28:1423-31.

[26] Cantor AB, Katz SG, Orkin SH. Distinct domains of the GATA-1 cofactor FOG-1 differentially influence erythroid versus megakaryocytic maturation. Mol Cell Biol 2002;22:4268-79.

[27] Terui K, Takahashi Y, Kitazawa J, Toki T, Yokoyama M, Ito E. Expression of transcription factors during megakaryocytic differentiation of CD34+ cells from human cord blood induced by thrombopoietin. Tohoku J Exp Med 2000;192:259-73.

[28] Hedrick L, Cho KR, Vogelstein B. Cell adhesion molecules as tumour suppressors. Trends Cell Biol 1993;3:36-9.

[29] Graff JR, Herman JG, Lapidus RG, Chopra H, Xu R, Jarrard DF, et al. E-cadherin expression is silenced by DNA hypermethylation in human breast and prostate carcinomas. Cancer Res 1995;55:5195-9.

[30] De Botton S, Sabri S, Daugas E, Zermati Y, Guidotti JE, Hermine O, et al. Platelet formation is the consequence of caspase activation within megakaryocytes. Blood 2002;100:1310-7.

[31] Shivdasani RA, Orkin SH. Erythropoiesis and globin gene expression in mice lacking the transcription factor NF-E2. Proc Natl Acad Sci U S A 1995;92:8690-4.

[32] Fujiwara Y, Chang AN, Williams AM, Orkin SH. Functional overlap of GATA-1 and GATA-2 in primitive hematopoietic development. Blood 2004;103:583-5.

[33] Sauntharajah Y, Hillery CA, Lavelle D, Molokie R, Dorn L, Bressler L, et al. Effects of 5-aza-2'-deoxycytidine on fetal hemoglobin levels, red cell adhesion, and hematopoietic differentiation in patients with sickle cell disease. Blood 2003;102:3865-70.

[34] Zermati Y, Garrido C, Amsellem S, Fishelson S, Bouscary D, Valensi F, et al. Caspase activation is required for terminal erythroid differentiation. J Exp Med 2001;193:247-54.

[35] Benito A, Silva M, Grillot D, Nunez G, Fernandez-Luna JL. Apoptosis induced by erythroid differentiation of human leukemia cell lines is inhibited by Bcl-XL. Blood 1996;87:3837-43.

[36] Socolovsky M, Fallon AE, Wang S, Brugnara C, Lodish HF. Fetal anemia and apoptosis of red cell progenitors in Stat5a-/-5b-/- mice: a direct role for Stat5 in Bcl-X(L) induction. Cell 1999;98:181-91.

[37] Gafni J, Cong X, Chen SF, Gibson BW, Ellerby LM. Calpain-1 cleaves and activates caspase-7. J Biol Chem 2009;284:25441-9.

[38] Demarchi F, Cataldo F, Bertoli C, Schneider C. DNA damage response links calpain to cellular senescence. Cell Cycle 2010;9:755-60.

[39] Yousefi S, Perozzo R, Schmid I, Ziemiecki A, Schaffner T, Scapozza L, et al. Calpain-mediated cleavage of Atg5 switches autophagy to apoptosis. Nat Cell Biol 2006;8:1124-32.

[40] Young AR, Narita M, Ferreira M, Kirschner K, Sadaie M, Darot JF, et al. Autophagy mediates the mitotic senescence transition. Genes Dev 2009;23:798-803.

**Table 1: List of human primer sequences used for mRNA expression analysis by real-time PCR.**

| Gene | Sequence (5'>3') | | Fragment length (bp) |
|---|---|---|---|
| | Forward | Reverse | |
| *β-actin* | CTCTTCCAGCCTTCCTTCCT | AGCACTGTGTTGGCGTACAG | 116 |
| *α-globin* | TCAAGCTCCTAAGCCACTGC | AGAAGCCAGGAACTTGTCCA | 101 |
| *β-globin* | CTGGGCAGATTACTGGTGGT | TTAGGGTTGCCCATAACAGC | 95 |
| *γ-globin* | CCCAGAGGTTCTTTGACAGC | GGAAGTCAGCACCTTCTTGC | 98 |
| *EpoR* | CTCATCCTCGTGGTCATCCT | CAGGCCAGATCTTCTGCTTC | 85 |
| *GATA1* | AGGCCACTACCTATGCAACG | CCTGCCCGTTTACTGACAAT | 105 |
| *GATA2* | CACAAGATGAATGGGCAGAA | GCCATAAGGTGGTGGTTGTC | 115 |
| *MafK* | TGATGAGCTGGTGTCCATGT | GTCACCTCCTCCTTGGTGAG | 72 |
| *NF-E2p45* | AATGCTCCAAGTGAGCCATC | AATCTGGGTGGATTGAGCAG | 100 |
| *CDH1* | CCTGGGACTCCACCTACAGA | CTGCTTGGATTCCAGAAACG | 108 |

*EpoR*: erythropoietin receptor, *NF-E2*: nucear factor-erythroid 2, *CDH1*: E-cadherin.

**Table 2. Effect of DAC exposure on K-562 and MEG-01 cell morphologies.**

| Cell line | DAC (days) | Size (Forward Scatter, a.u.) | Granularity (Side Scatter, a.u.) | Average cell size (µM) |
|---|---|---|---|---|
| K-562 | 0 | 355±5 | 367±7 | 14.4±0.3 |
| | 1 | 362±5 | 385±6 * | 14.4±0.4 |
| | 2 | 375±8 * | 427±13 ** | 16.8±0.4 ** |
| | 3 | 383±3 ** | 465±23 ** | 18.2±0.7 ** |
| | 4 | 389±2 ** | 570±23 ** | 20.4±0.9 ** |
| | 6 | 397±5 ** | 710±17 ** | 22.9±1.4 ** |
| | 6 | 401±2 ** | 763±20 ** | 25.5±0.8 ** |
| | 10 | 407±2 ** | 857±17 ** | 27.5±1.1 ** |
| | 13 | 416±4 ** | 943±15 ** | ND |
| MEG-01 | 0 | 314±9 | 341±8 | 12.5±0.3 |
| | 1 | 315±4 | 342±9 | 12.9±0.3 |
| | 2 | 322±7 | 387±9 ** | 13.4±0.2 ** |
| | 3s | 325±7 | 412±13 ** | 13.4±0.3 ** |
| | 3a | ND | 397±5 ** | 14.9±0.2 **, ## |
| | 4s | 333±6 * | 450±13 ** | 14.7±0.3 ** |
| | 4a | ND | 427±5 ** | 15.5±0.4 **, # |
| | 6s | 337±4 * | 515±6 ** | 15.1±0.4 ** |
| | 6a | ND | 573±15 **, # | 18.5±0.5 **, ## |
| | 8s | 341±8 * | 546±16 ** | 15.5±0.4 ** |
| | 8s | ND | 637±11 **, ## | 20.2±0.9 **, ## |
| | 10s | 347±7 ** | 571±11 ** | ND |
| | 10a | ND | 677±22 **, ## | ND |

K-562 and MEG-01 cells were treated with 2 µM DAC. At various time points, cells were collected and analyzed either by flow cytometry (FACS, Becton Dickinson) using forward (relative cell sizes) and side scatter (granularity) measurements or using a semi-automated image-based cell analyzer (average cell size). Data were analyzed to exclude debris. Results are the mean (±SD) of three independent experiments. * and ** indicate $p<0.05$ and $p<0.01$ versus control, respectively. # and ## indicate $p<0.05$ and $p<0.01$ versus suspension cells. ND: not determined.

**Titles and legends to figures**

**Figure 1. Biologic response of human CML K-562 and MEG-01 cells to DAC treatment.**

K-562 and MEG-01 cells were grown for various times in a medium supplemented with 2 µM DAC. (A) Cell viability was evaluated by Trypan blue exclusion staining. Data are the mean (±SD) of three independent experiments. (B) Microscopy pictures from typical morphologies observed after DAC treatment. Pictures from a typical experiment representative of three. Original magnification, X400. Arrows indicate vacuoles in K-562 cells and adherent cells in MEG-01 cell line. (D) The percentage of cells adhering to the plastic dish was evaluated by scoring the number of cells that needed trypsinization to be detached from the plate compared to the number of cells growing in suspension. Data are the mean (±SD) of three independent experiments. * and ** indicate $p<0.05$ and $p<0.01$ versus control, respectively.

**Figure 2. Effect of DAC on DNMT1 levels and global DNA methylation in K-562 and MEG-01 cells.**

K-562 and MEG-01 cells were cultured in a medium supplemented of 2 µM DAC. (A) After 4 days, total proteins were isolated and analyzed by western blot for DNMT1 expression levels. β-actin was used as a loading control. (B) At various time points, cells were collected, genomic DNA extracted, and global DNA methylation assessed by MSRA. *Msp*I- and *Hpa*II-digested DNA was resolved on a 0.8% agarose gel and visualized by ethidium bromide staining. Undigested genomic DNA was used as a control. Pictures are representative of three independent experiments.

**Figure 3. DAC induces erythroid differentiation of K-562 cells and megakaryocytic differentiation of MEG-01 cells in a time-dependent manner.**

K-562 and MEG-01 cells were grown in a medium with 2 µM DAC. (A) Upper panel: K-562 cell pellets of untreated and DAC-treated cells were photographed after 6 days to show the development of red pigmentation in treated cells. Lower panel: The percentage of hemoglobin producing cells was assessed by benzidine staining at various time points after addition of DAC. A picture of untreated and DAC-treated cells is shown. (B) Flow cytometry analysis of megakaryocytic surface markers CD41, CD61 and the erythroid surface marker glycophorin A (GPA) after 4 days of culture in K-562 (left panel) and in total MEG-01 population (right panel). (C) Flow cytometry analysis of surface markers CD41, CD61 and GPA at various time points in DAC-treated K-562 and MEG-01 cells. Suspension (s) and adherent (a) MEG-01 populations were analyzed separately after 3 days of treatment. (D) Forward and side scatter plots showing that DAC-treated MEG-01 cells are able after 4 days of treatment to produce particles similar to freshly isolated human platelets (upper panel). Direct immunostaining using FITC-conjugated CD61 antibody and flow cytometry analysis showed that MEG-01-derived particles expressed the platelet surface marker CD61 (lower panel). After 4 days of treatment, MEG-01 cells were analyzed for CD61 expression by flow cytometry compared to isotype-match negative control, and reported as a relative mean fluorescence intensity (MFI). Dot plots are representative of three independent experiments. Total RNA was extracted from K-562 (E) and MEG-01 (F) cells treated with 2 µM DAC at various time points, then reverse transcribed and real-time PCR was used to analyze mRNA expression level of indicated genes. Adherent (a) and suspension (s) MEG-01 populations were analyzed separately from 3 days of treatment. Gene expression was normalized to β-actin. Data are the mean (±SD) of three independent experiments. In all experiments, * and ** indicate $p<0.05$ and $p<0.01$ versus control, respectively. $ indicates a statistical trend ($p<0.10$). GPA: glycophorin A, EpoR: erythropoietin receptor, NF-E2: Nuclear factor-erythroid 2, CDH1: E-cadherin.

**Figure 4. DAC promotes the expression of senescence and autophagic markers in K-562 and MEG-01 cells.**

K-562 and MEG-01 cells were incubated in a medium with 2 µM DAC for 4 days. Adherent (a) and suspension (s) MEG-01 populations were analyzed separately. (A) Pictures of cells stained with X-gal. K-562 treated with 120 nM of doxorubicin for 4 days were used as a positive control. Senescence-associated β-galactosidase activity is revealed by an increase in blue staining. (B) Senescent cells were expressed as a percentage of the total number of cells counted (lower panel). Data represent the mean (±SD) of three independent experiments. ** indicates $p<0.01$ versus control. (C) Total proteins were extracted and analyzed by western blot for LC3 conversion as a marker of autophagy. β-actin was used as a loading control. (D) Electron microphotographs of untreated and DAC-treated K-562 and adherent MEG-01 cells. Pictures show double-layered membrane-bounded autophagosomes enclosing cell constituents (arrows). Pictures are representative of three independent experiments. LC3: light chain 3.

**Figure 5. Long-time DAC exposure engaged the CML K-562 and MEG-01 cell lines into the intrinsic pathway of apoptosis.**

K-562 and MEG-01 cells were treated with 2 µM DAC and apoptosis was evaluated after various times of incubation. (A) Cells were stained with Hoechst and PI followed by fluorescence microscopic observation with an IX81 (MT10) Olympus microscope. Pictures are representative of three independent experiments. (B) Number of apoptotic cells as a percentage of the total number of cells counted. Adherent (a) and suspension (s) MEG-01 populations were analyzed separately. Data are the mean (±SD) of three independent cultures. (C) Cells were stained for Annexin V/PI and analyzed by flow cytometry to follow

phosphatidyl serine externalization. Dot plots are representative of three independent experiments. The percentage of cells positive for each marker is indicated. Data represent the mean (±SD) of three independent experiments. (C) Total proteins were isolated and analyzed by western blot for caspase activation and PARP cleavage. (D) Total proteins were isolated and analyzed by western blot for the expression of key pro- and anti-apoptotic proteins. β-actin was used as a loading control. U-937 cells left untreated (-) or treated with 100 µM etoposide for 4 h (+) were used as controls of apoptosis and caspase cleavage. Adherent (a) and suspension (s) MEG-01 populations were analyzed separately. Blots are representative results of three independent experiments. Bcl-2: B-cell lymphoma 2, Mcl-1: Myeloid cell leukemia-1, PARP: poly ADP ribose polymerase, XIAP: X-linked inhibitor of apoptosis protein.

**Figure 6. DAC induces calpain activity in K-562 and MEG-01 leukemia cell lines.**

K-562 and MEG-01 cells were treated with 2 µM DAC. At various time points, cells were collected to assess calpain activity. Fluoresence intensity was measured and reported to the protein quantity and then expressed as relative fluorescence units (RFU). Adherent (a) and suspension (s) MEG-01 populations were analyzed separately. Data are the mean (±SD) of three independent experiments. * and ** indicate $p<0.05$ and $p<0.01$ versus control, respectively. $^{\#}$ and $^{\#\#}$ indicate $p<0.05$ and $p<0.01$ versus suspension cells.

**Figure 7. DAC-induced differentiation sensitizes CML cell lines to both conventional chemotherapeutic drugs and HDACi.**

(A) K-562 and MEG-01 cells were left untreated or pre-treated with 2 µM DAC for 3 days and then treated or not with 10 µM and 25 µM cisplatin or etoposide for 24h. Cells were stained with Hoechst and PI, and apoptosis was evaluated by fluorescence microscopic observation. (B) K-562 cells were treated with DAC or SAHA alone, or in combination for

the indicated period of time, and apoptosis was determined using Hoechst/PI staining. Data are the mean (±SD) of three independent experiments. (C) PBMCs were isolated from fresh buffy coats of four healthy adult human donors and treated with DMSO (vehicle control), 2 µM DAC, 2 µM SAHA, 10 µM cisplatin (Cis10), 25 µM cisplatin (Cis25), 10 µM etoposide (Eto10), or 25 µM etoposide (Eto25) alone, or in combination for the indicated period of time. Cell viability was evaluated by Trypan blue exclusion staining. Data are the mean (±SD) of three independent experiments.

*Graphical Abstract

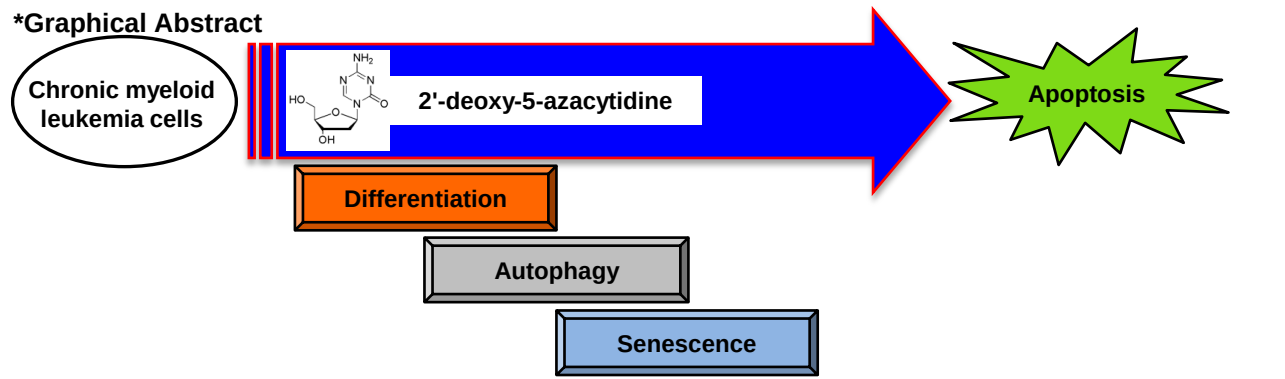

Fig. 1

A

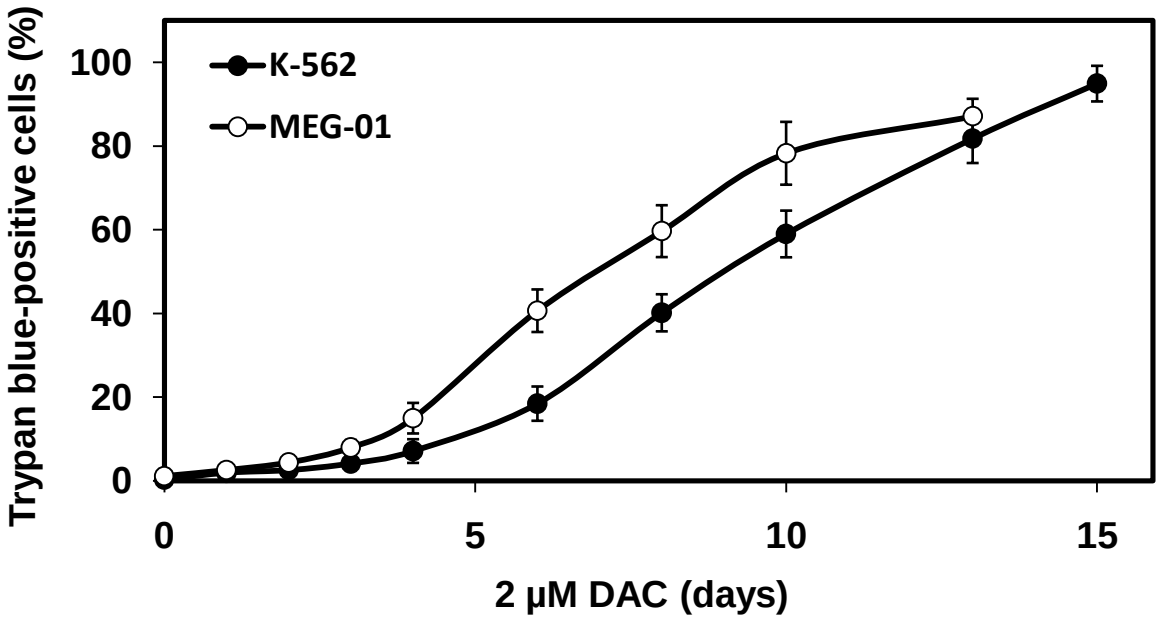
Trypan blue-positive cells (%)
100
80
60
40
20
0
K-562
MEG-01
0
5
10
15
2 μM DAC (days)

B

K-562

DAC (days)

0

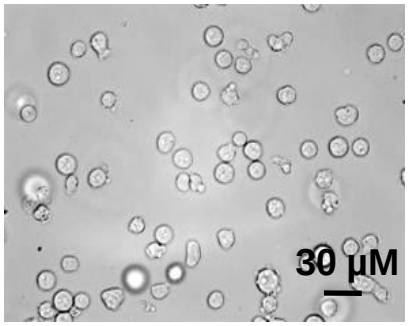


1

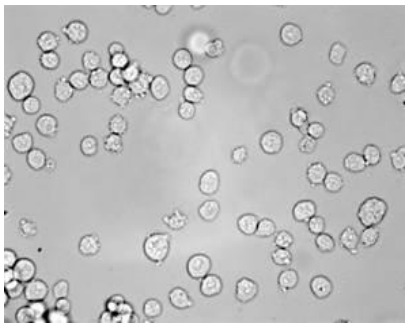

2

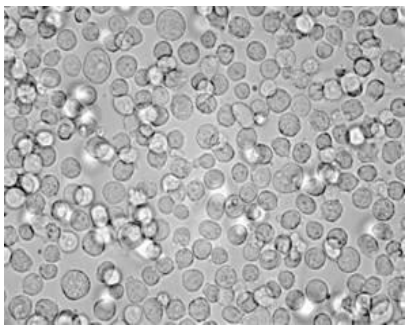

3

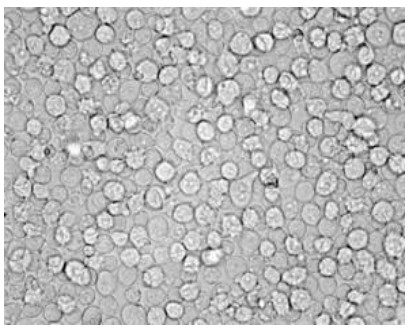

4

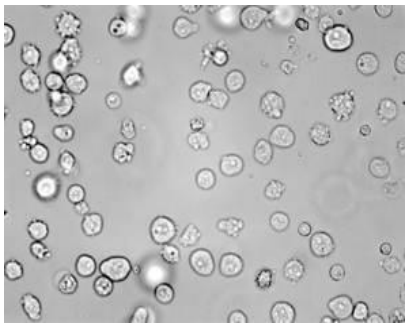

DAC (days)

6

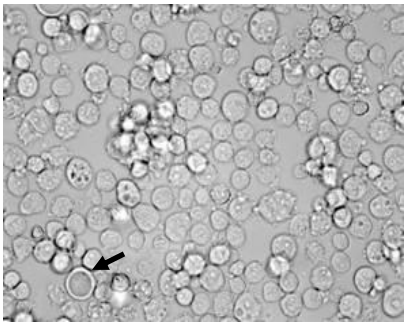

8

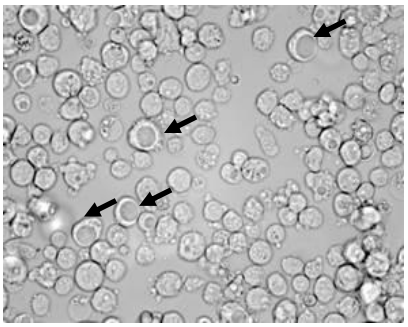

10

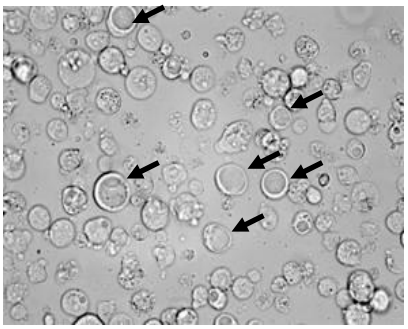

B

MEG-01

DAC (days)

0

1

2

3

DAC (days)

4

6

8

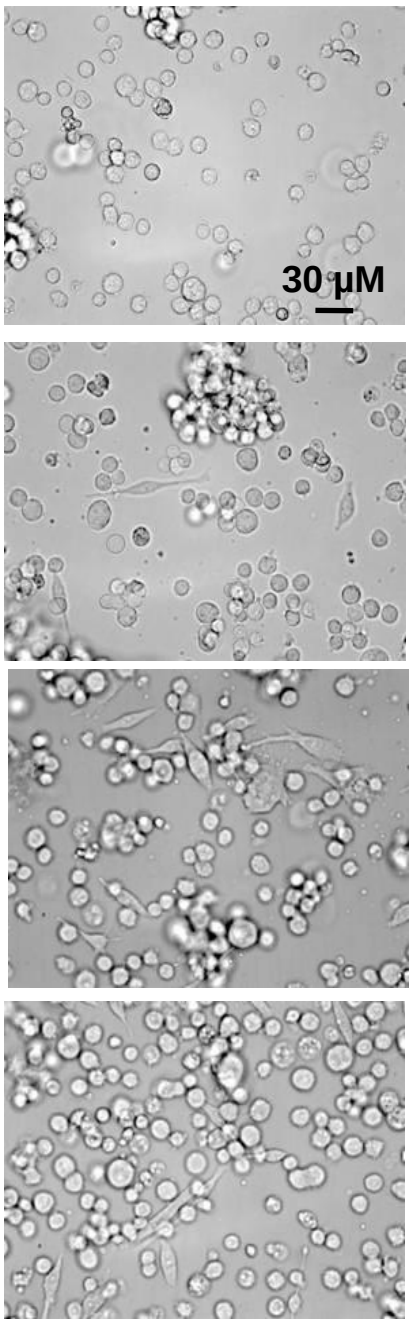

C

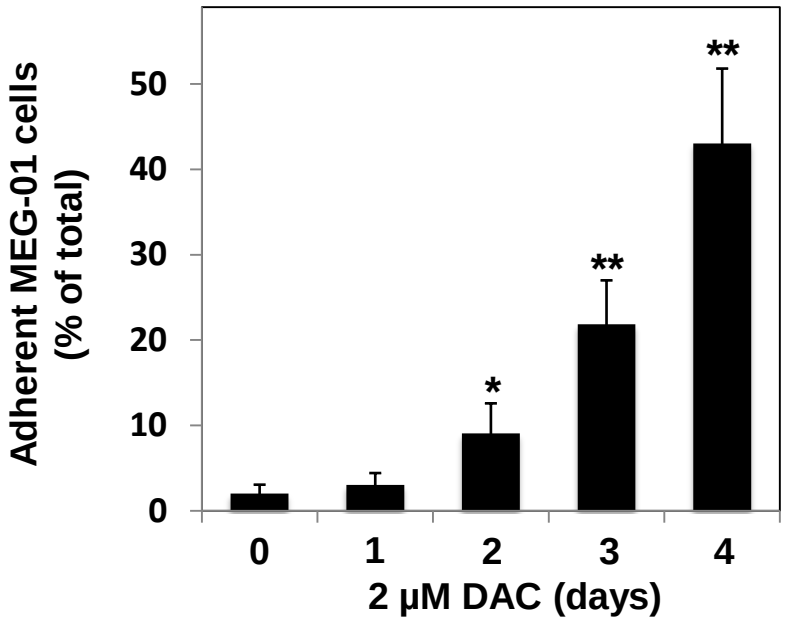
Adherent MEG-01 cells
(% of total)
50
40
30
20
10
0
*
**
**
0
1
2
3
4
2 µM DAC (days)

A

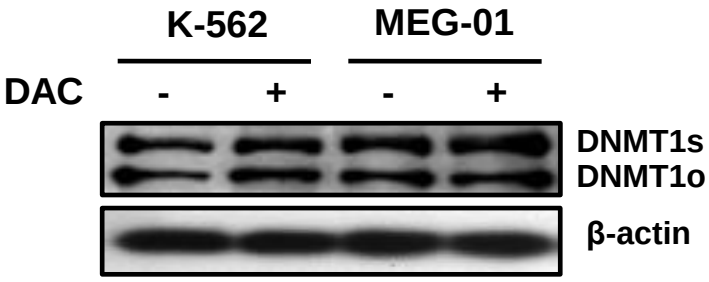
K-562
MEG-01
DAC
-
+
-
+
DNMT1s
DNMT1o
β-actin

B

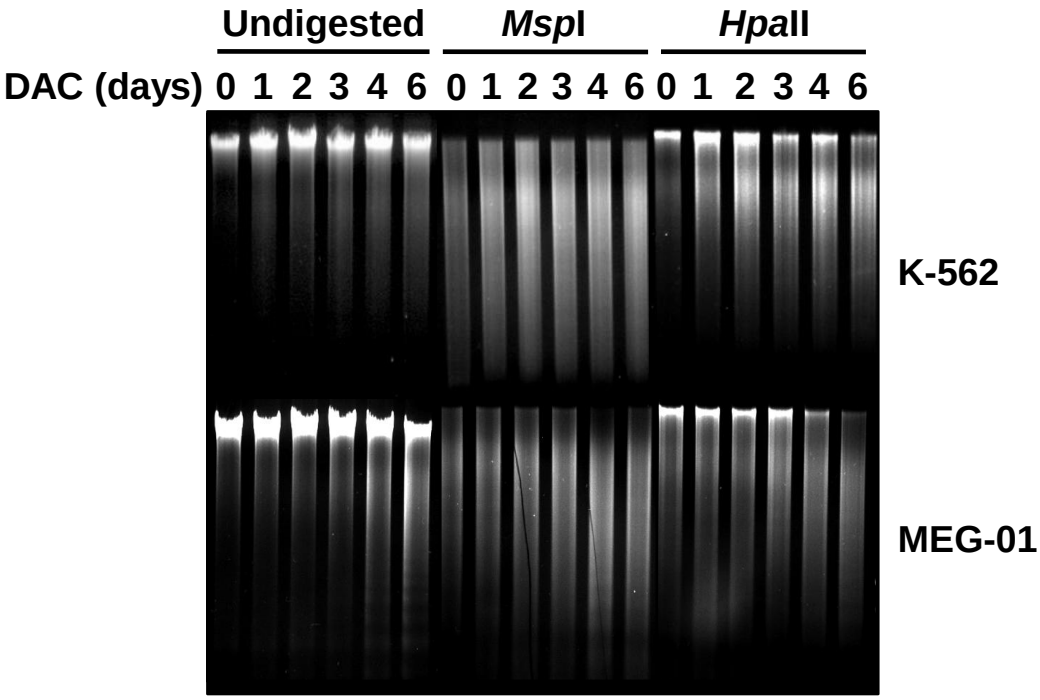
Undigested
MspI
HpaII
DAC (days) 0 1 2 3 4 6 0 1 2 3 4 6 0 1 2 3 4 6
K-562
MEG-01

Fig. 3

A

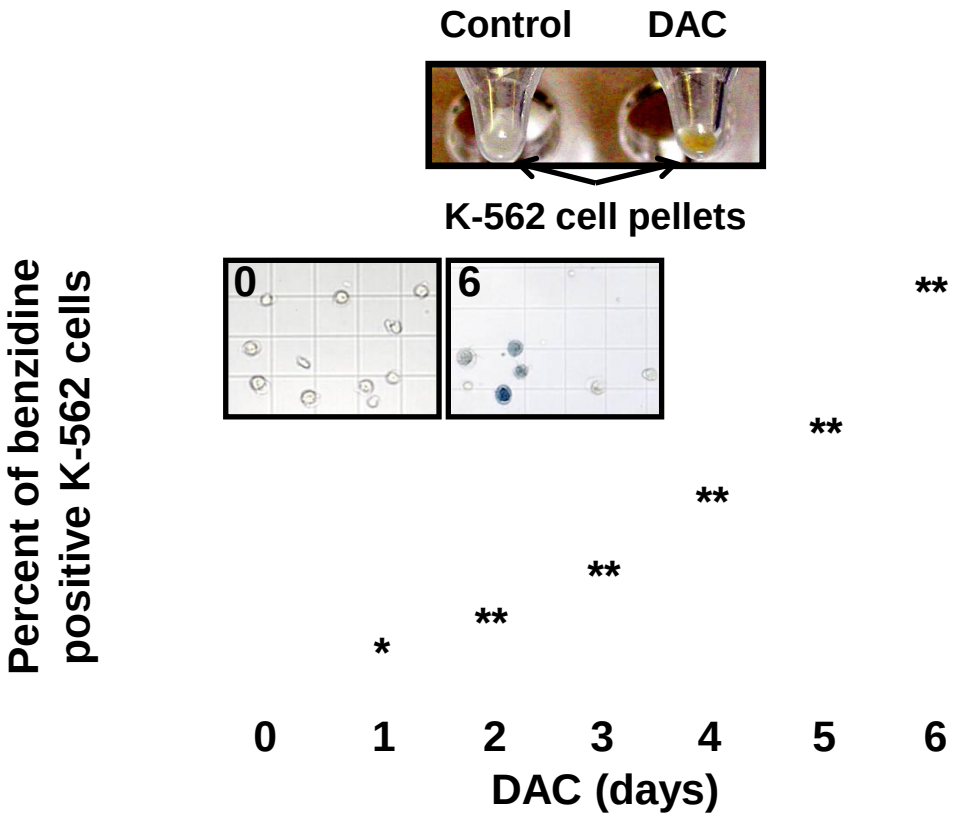
Control
DAC
K-562 cell pellets
0
6
Percent of benzidine positive K-562 cells
*
**
**
**
**
**
0
1
2
3
4
5
6
DAC (days)

B

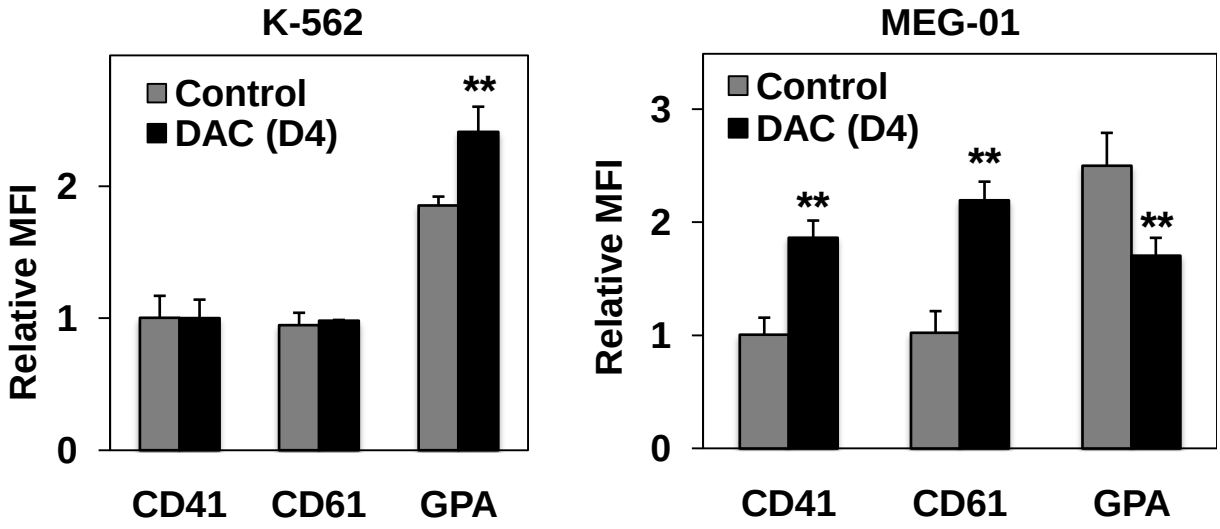
K-562
Control
DAC (D4)
Relative MFI
0
1
2
**
CD41
CD61
GPA
MEG-01
Control
DAC (D4)
Relative MFI
0
1
2
3
**
**
**
CD41
CD61
GPA

C

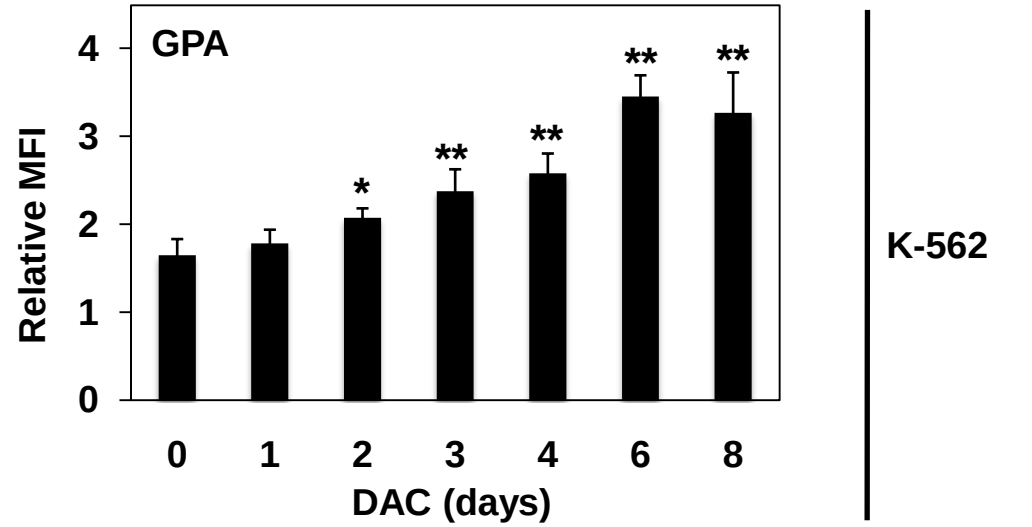
GPA
Relative MFI
0
1
2
3
4
0 1 2 3 4 6 8
DAC (days)

K-562

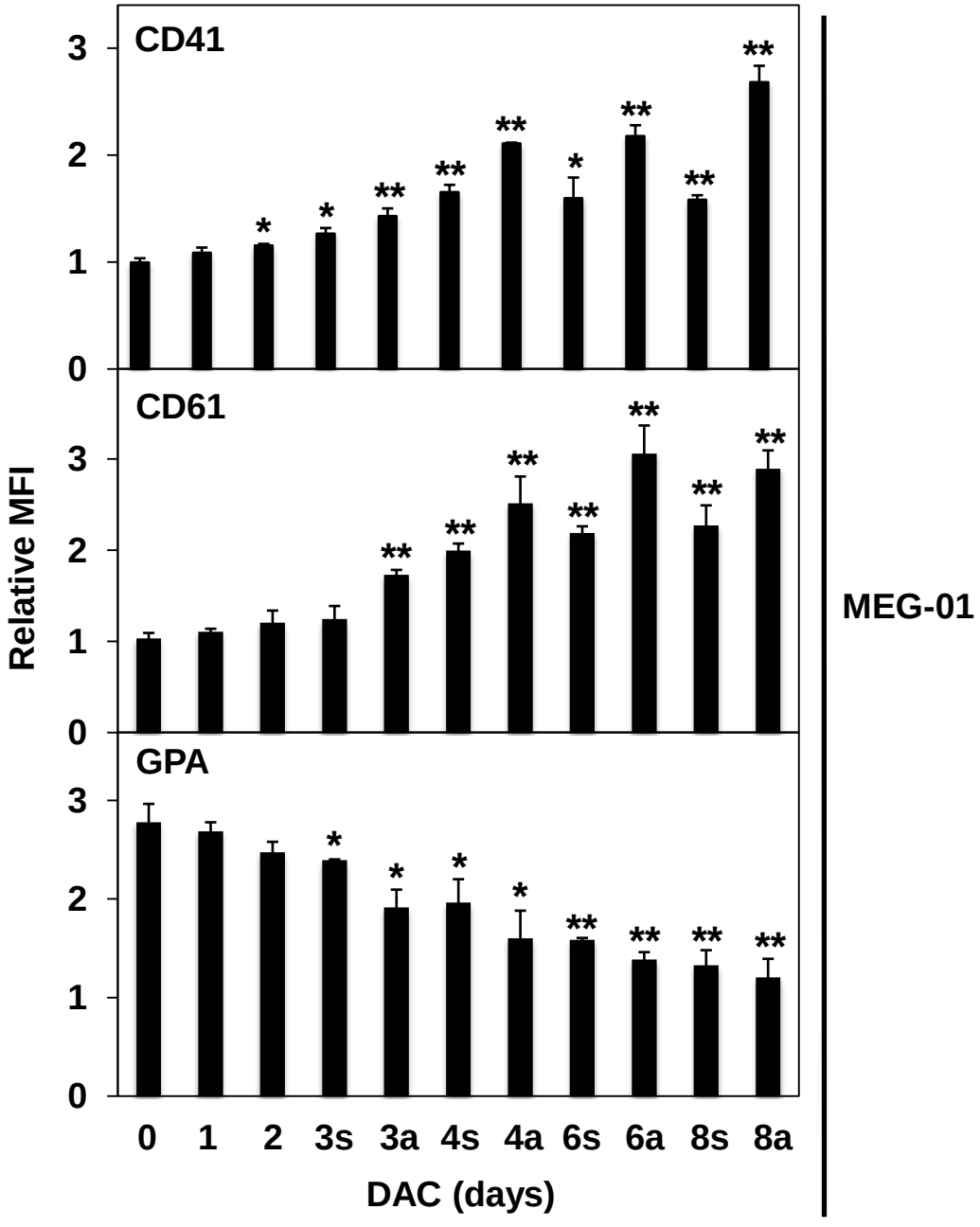
CD41
CD61
GPA
Relative MFI
0 1 2 3
0 1 2 3s 3a 4s 4a 6s 6a 8s 8a
DAC (days)

MEG-01

D

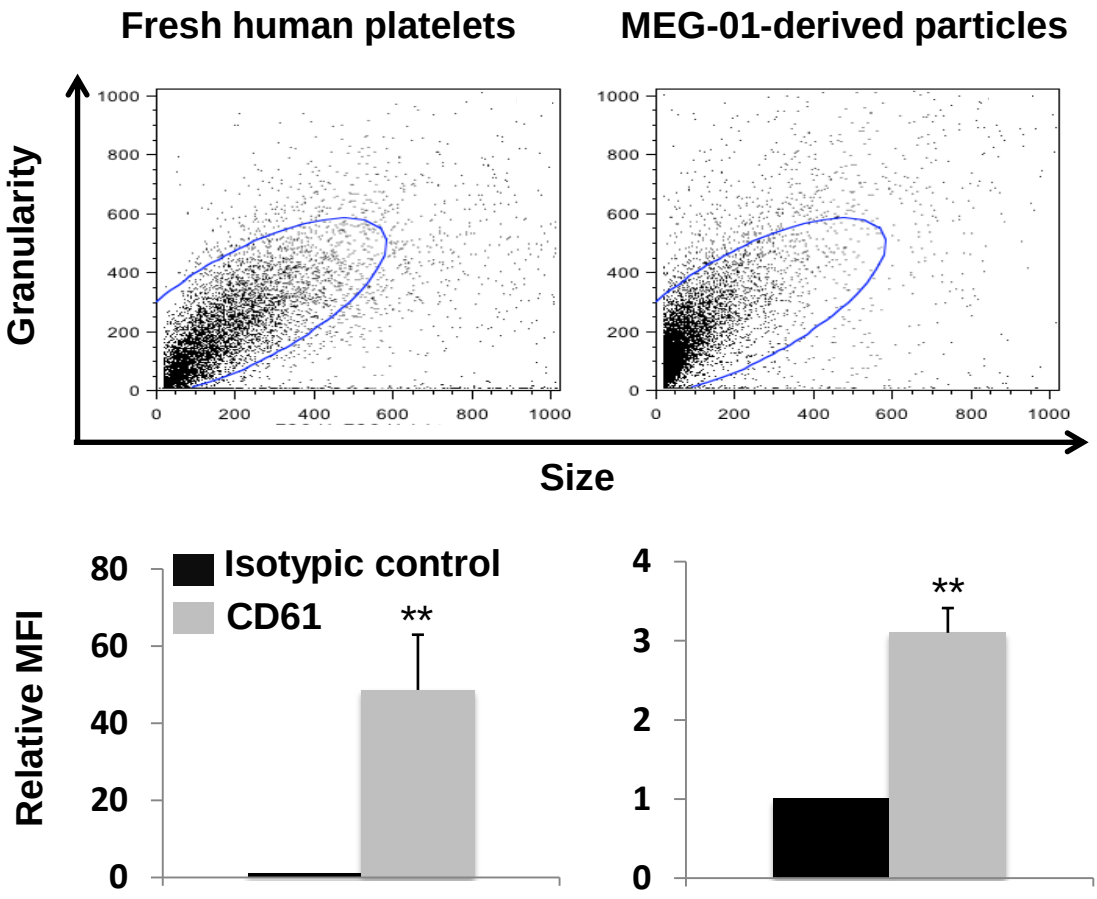
Fresh human platelets
MEG-01-derived particles
Granularity
Size
0
200
400
600
800
1000
Relative MFI
Isotypic control
CD61
**
**
0
20
40
60
80
0
1
2
3
4

E

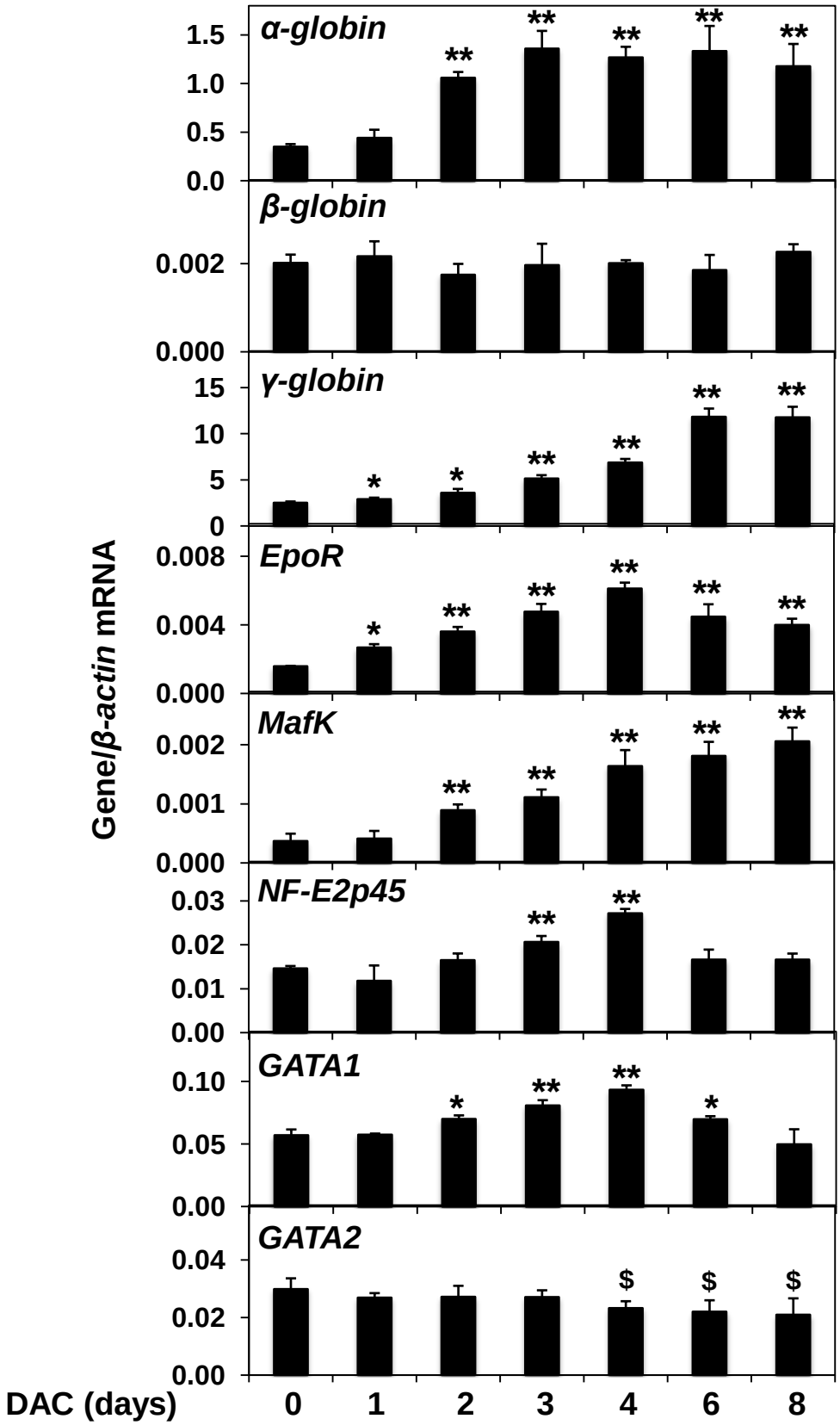
α-globin
β-globin
γ-globin
EpoR
MafK
NF-E2p45
GATA1
GATA2
Gene/β-actin mRNA
DAC (days)
0
1
2
3
4
6
8

F

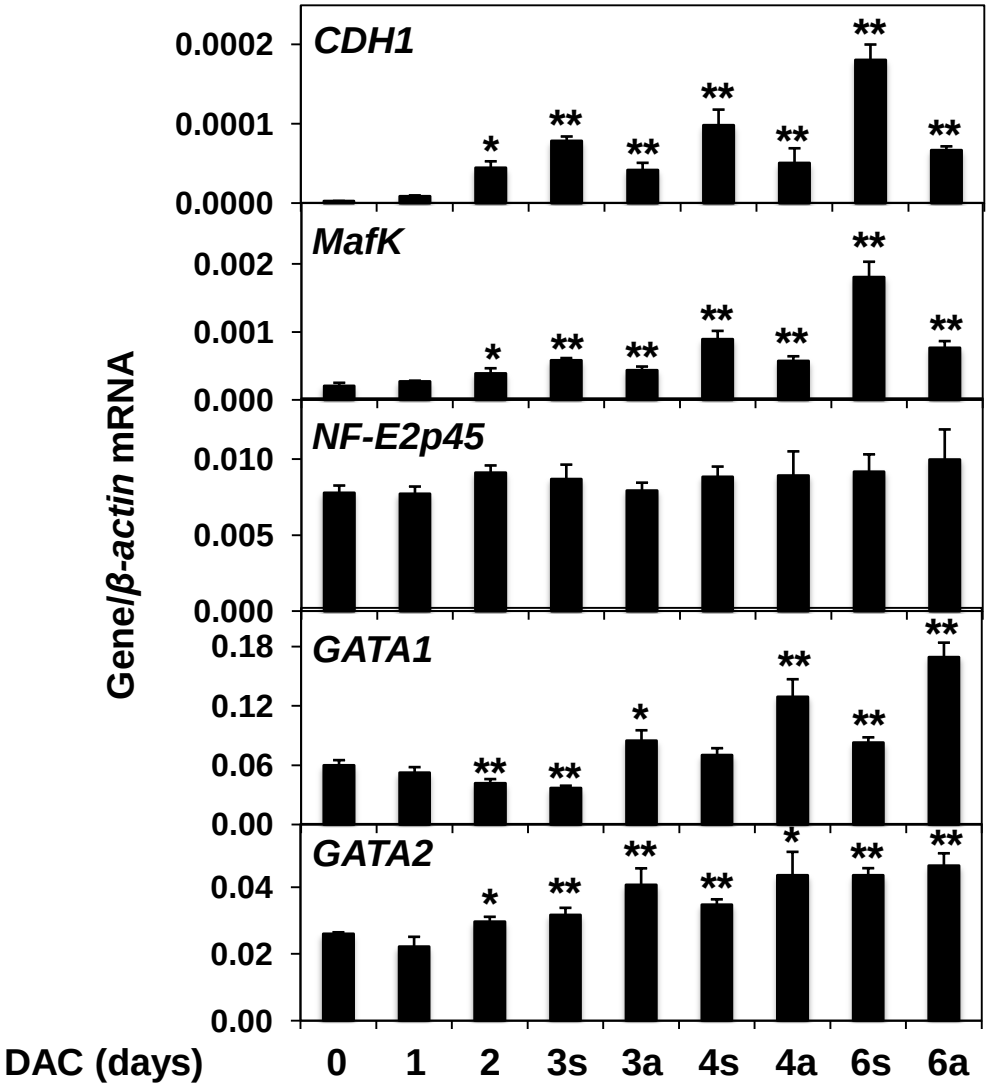
CDH1
MafK
NF-E2p45
GATA1
GATA2
Gene/β-actin mRNA
0.0002
0.0001
0.0000
0.002
0.001
0.000
0.010
0.005
0.000
0.18
0.12
0.06
0.00
0.04
0.02
0.00
DAC (days)
0
1
2
3s
3a
4s
4a
6s
6a

Figure intended for color reproduction on the Web and in print

Fig. 4

A

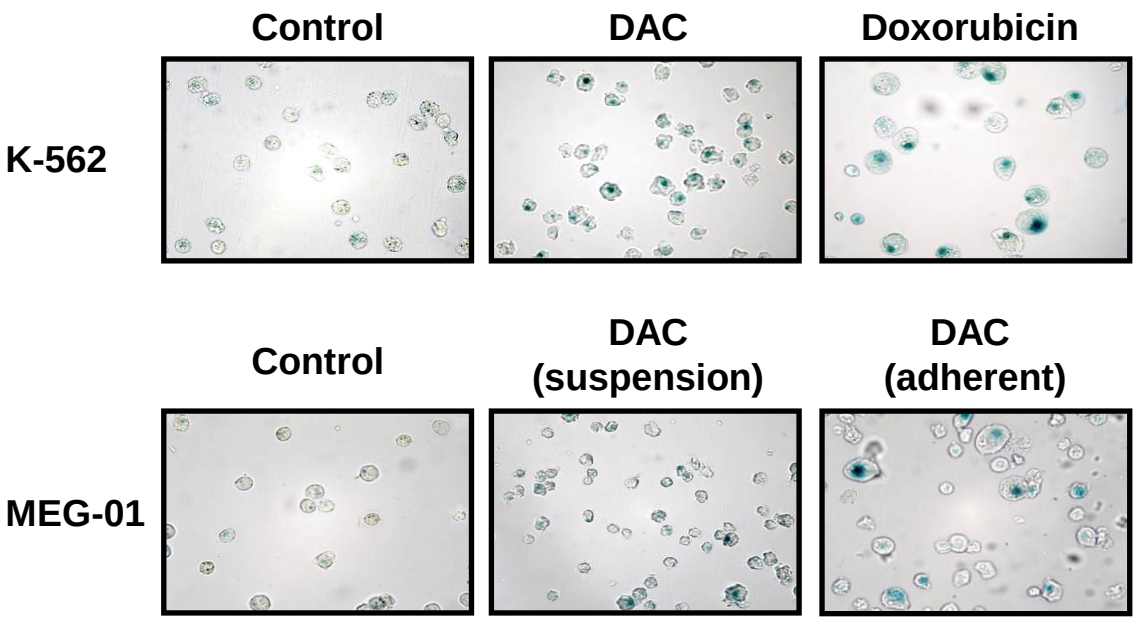


B

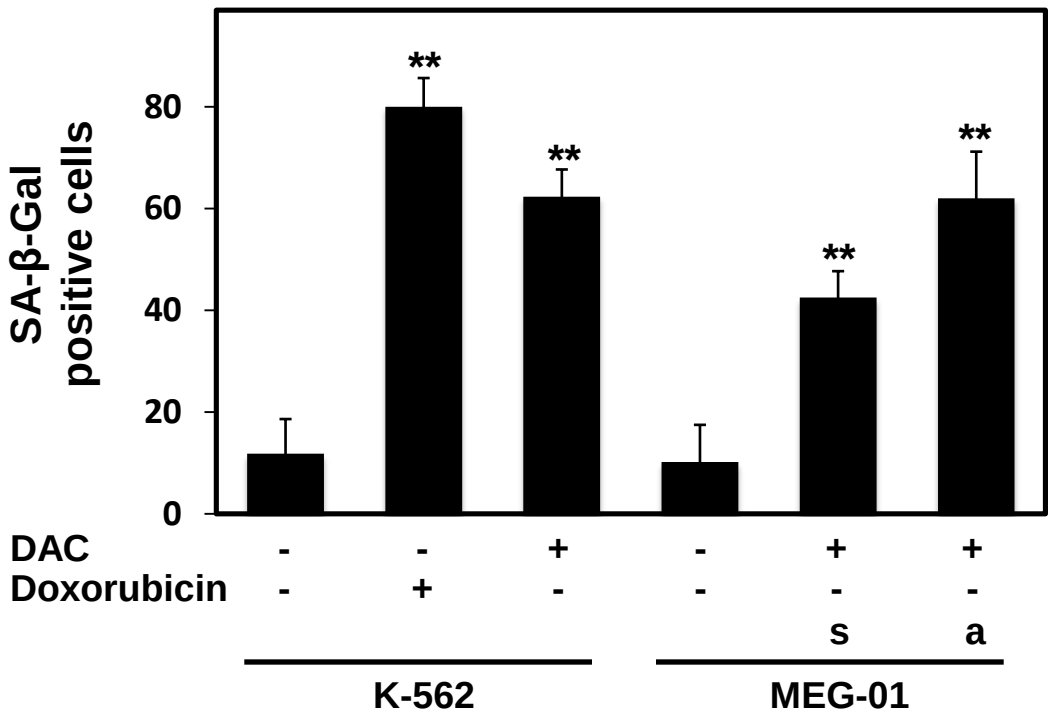

C

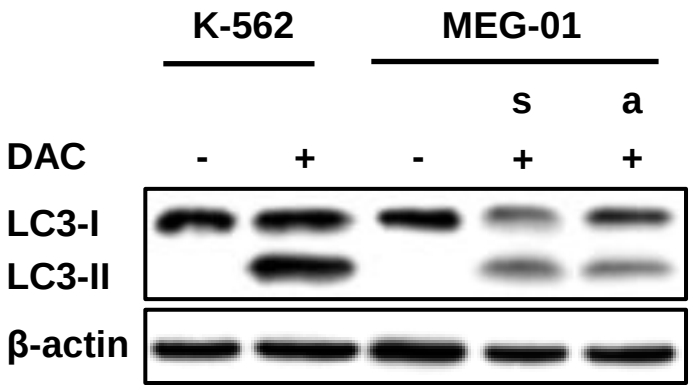
K-562
MEG-01
s
a
DAC
-
+
-
+
+
LC3-I
LC3-II
β-actin

D

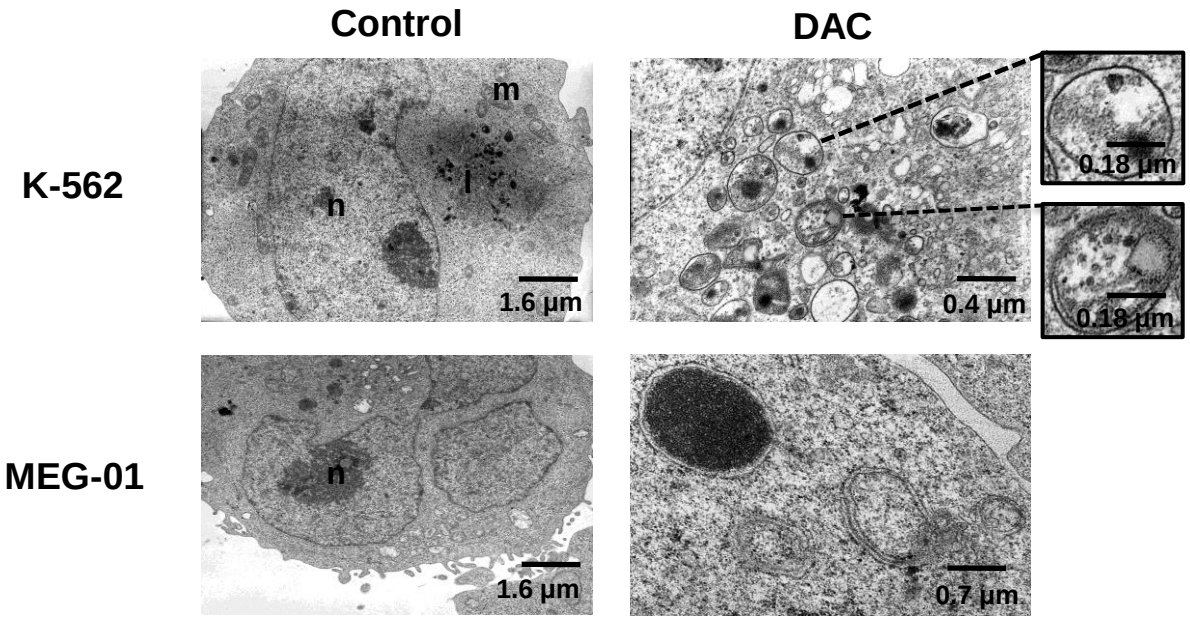
Control
DAC
K-562
MEG-01
m
l
n
n
1.6 μm
1.6 μm
0.4 μm
0.18 μm
0.18 μm
0.7 μm

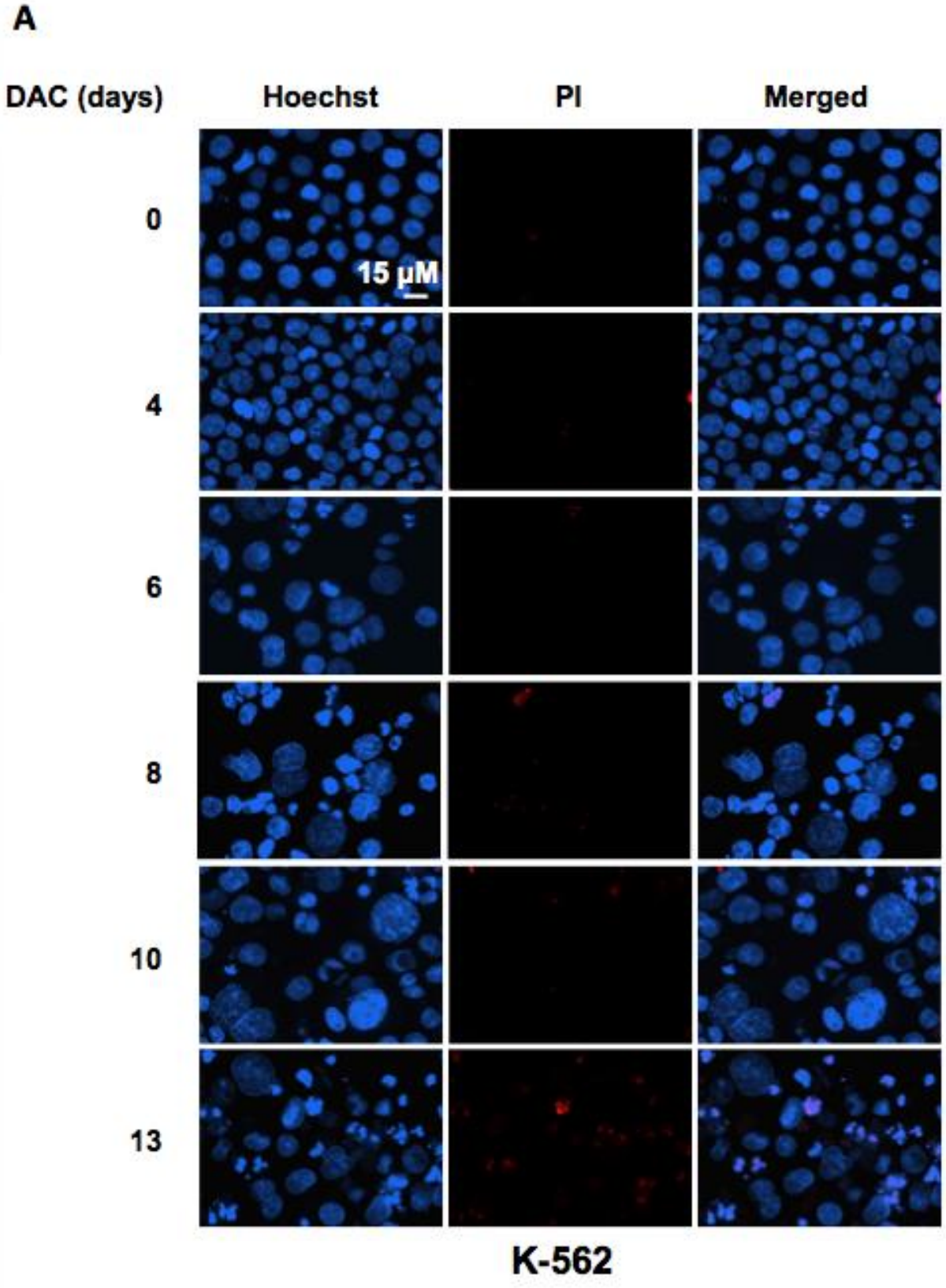
A
DAC (days)
Hoechst
PI
Merged
0
4
6
8
10
13
15 µM
K-562

Figure intended for color reproduction on the Web and in print

Fig. 5

A

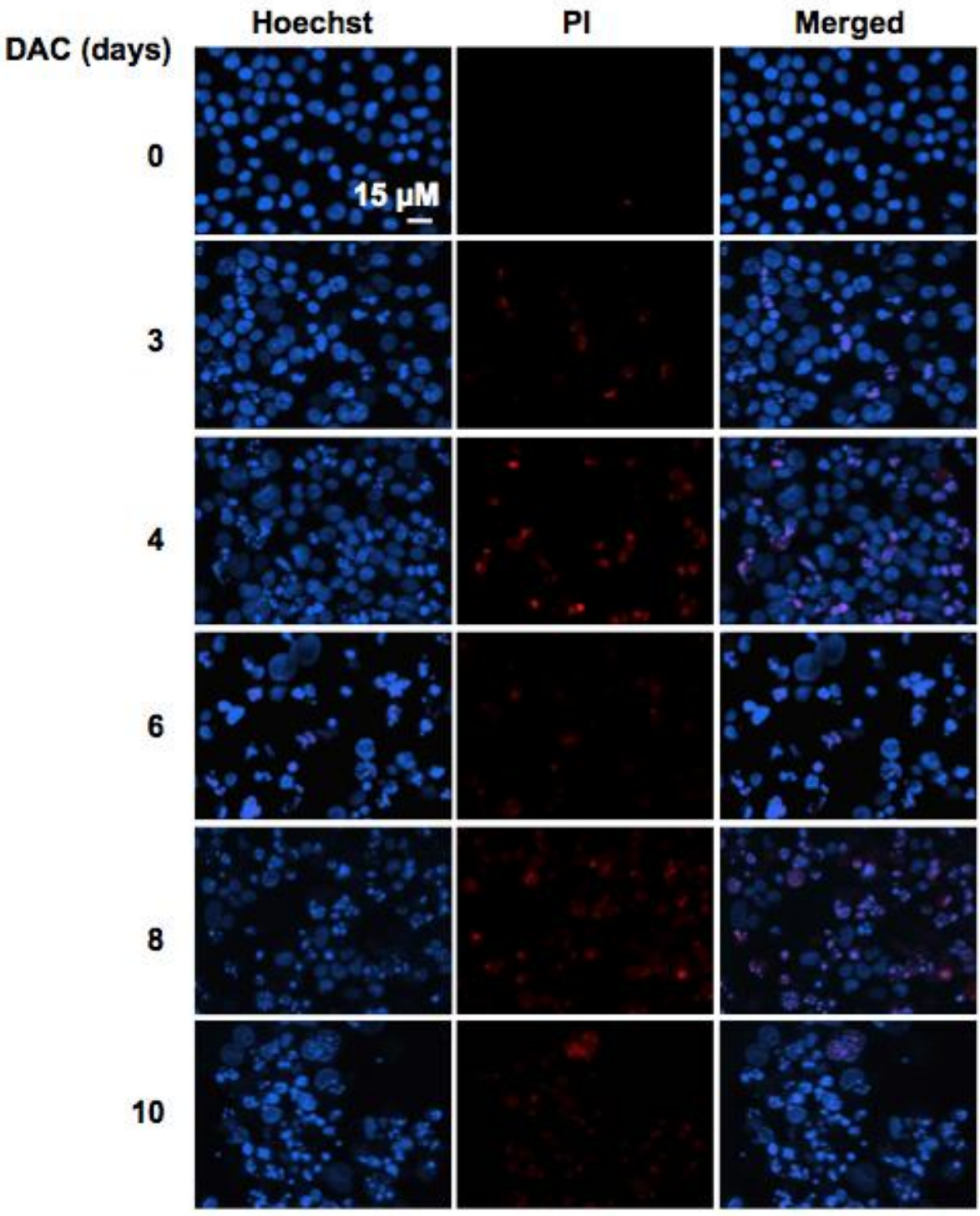

Figure intended for color reproduction on the Web and in print

Fig. 5

A

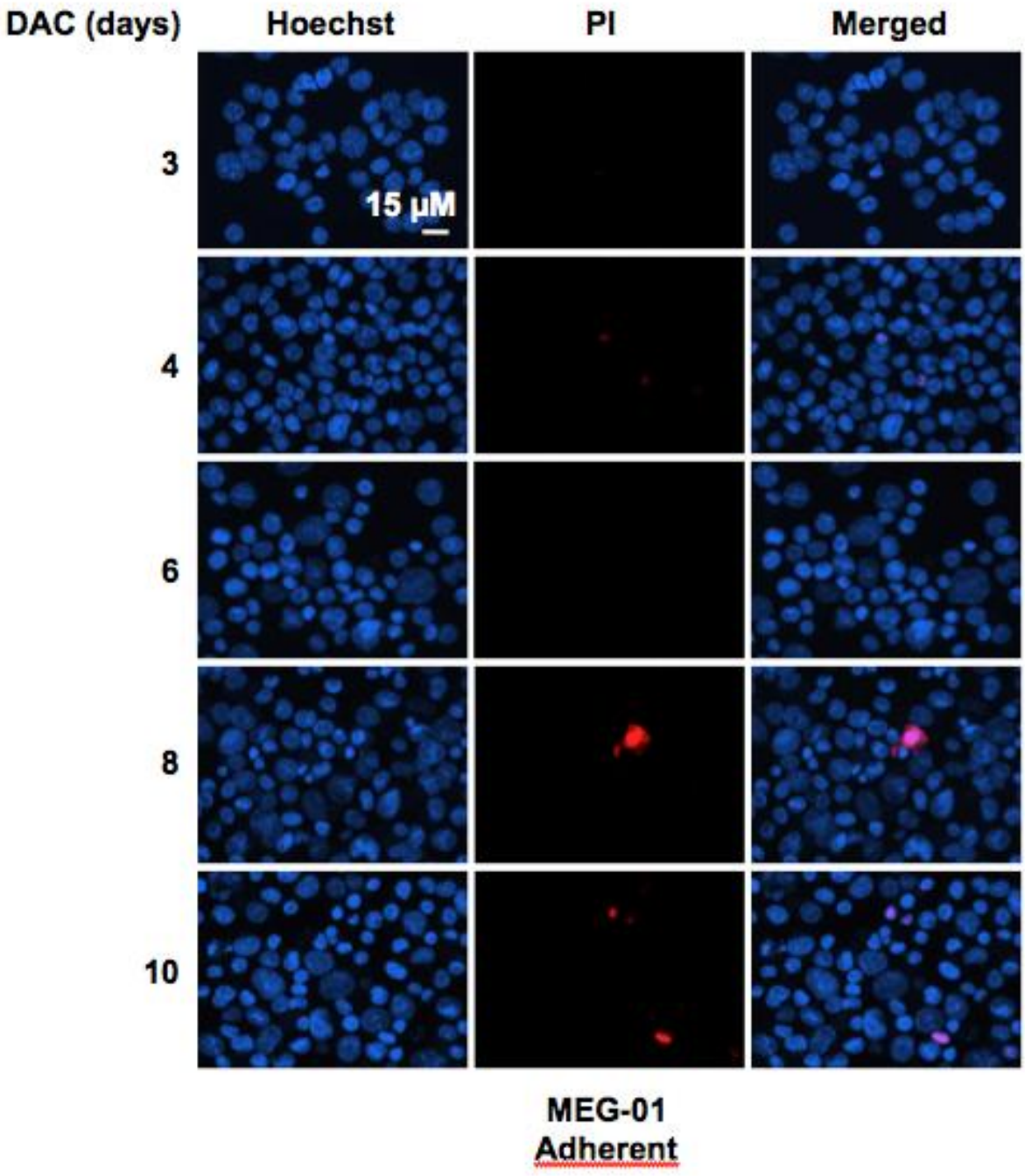

B

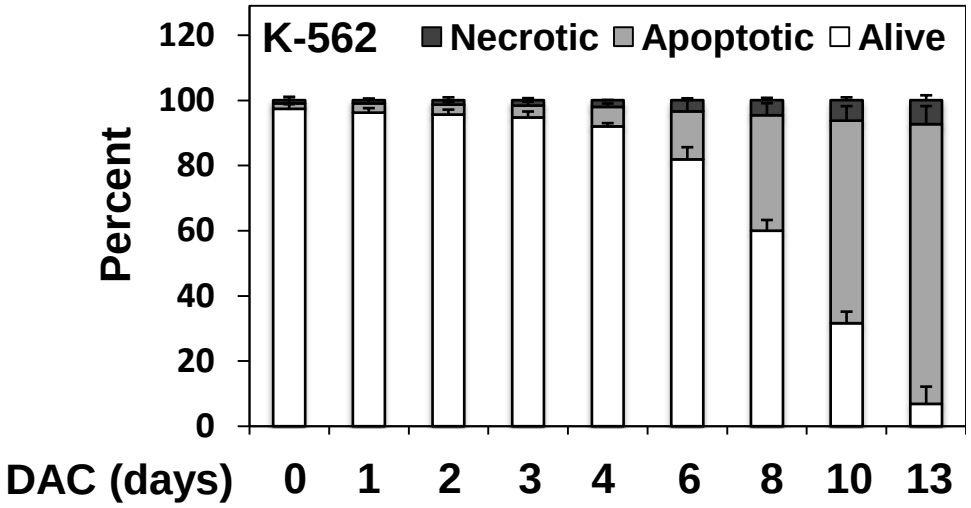
K-562
Necrotic
Apoptotic
Alive
Percent
120
100
80
60
40
20
0
DAC (days)
0
1
2
3
4
6
8
10
13

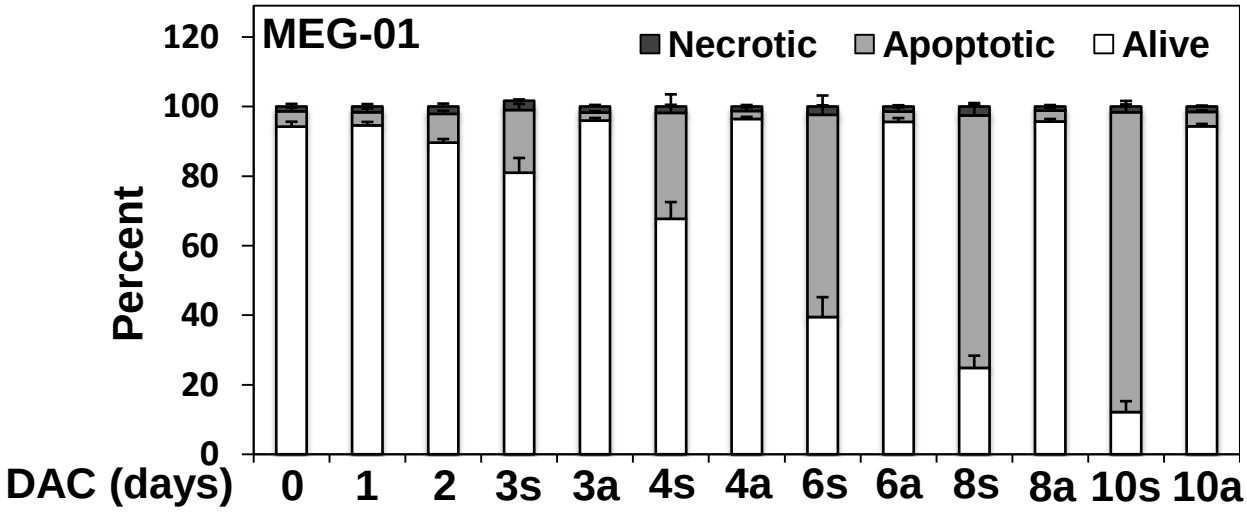
MEG-01
Necrotic
Apoptotic
Alive
Percent
120
100
80
60
40
20
0
DAC (days)
0
1
2
3s
3a
4s
4a
6s
6a
8s
8a
10s
10a

C

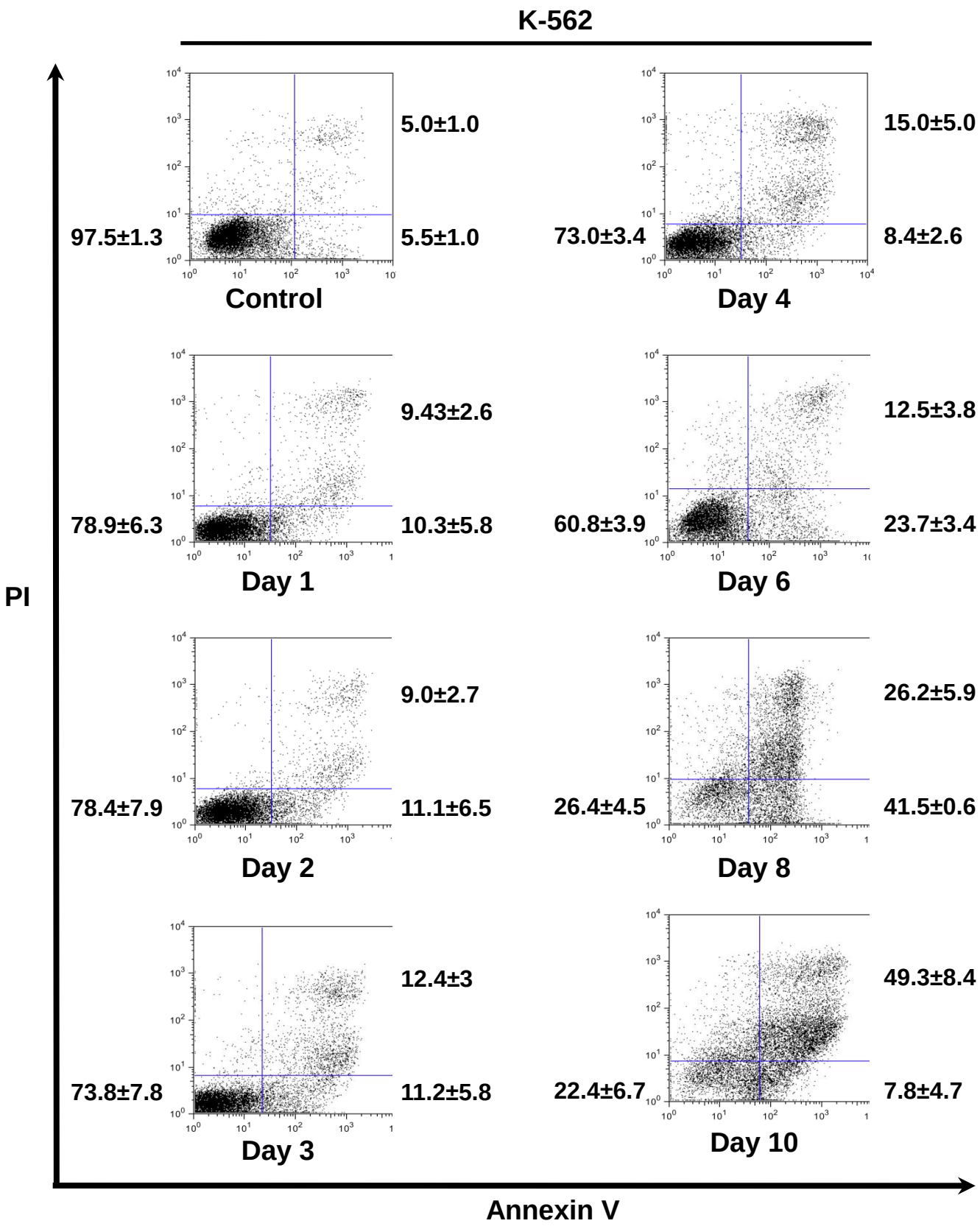
K-562
PI
Annexin V
97.5±1.3
5.0±1.0
5.5±1.0
Control
73.0±3.4
15.0±5.0
8.4±2.6
Day 4
78.9±6.3
9.43±2.6
10.3±5.8
Day 1
60.8±3.9
12.5±3.8
23.7±3.4
Day 6
78.4±7.9
9.0±2.7
11.1±6.5
Day 2
26.4±4.5
26.2±5.9
41.5±0.6
Day 8
73.8±7.8
12.4±3
11.2±5.8
Day 3
22.4±6.7
49.3±8.4
7.8±4.7
Day 10

C

MEG-01

Suspension | Adherent | Suspension

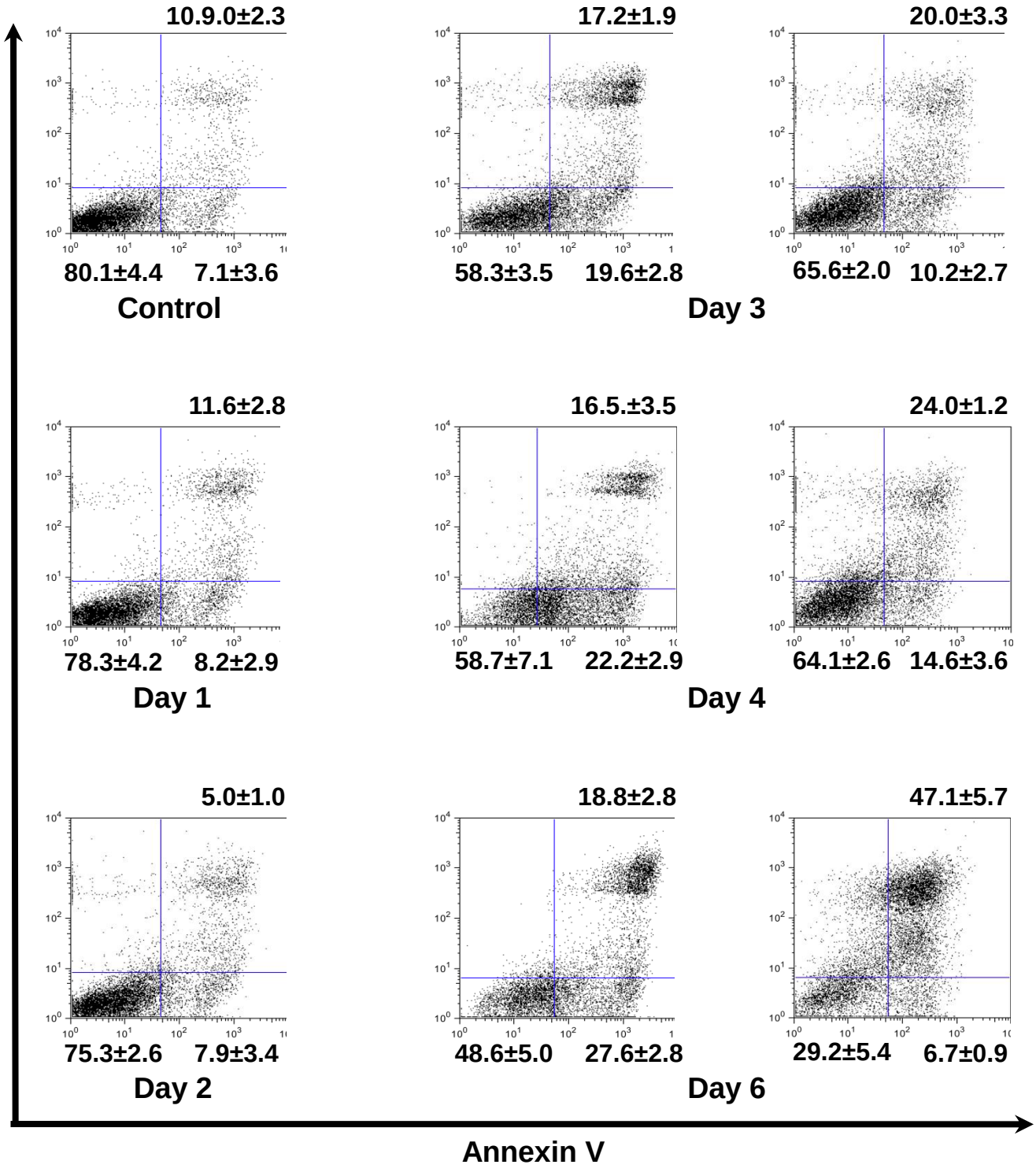

Fig. 5

D

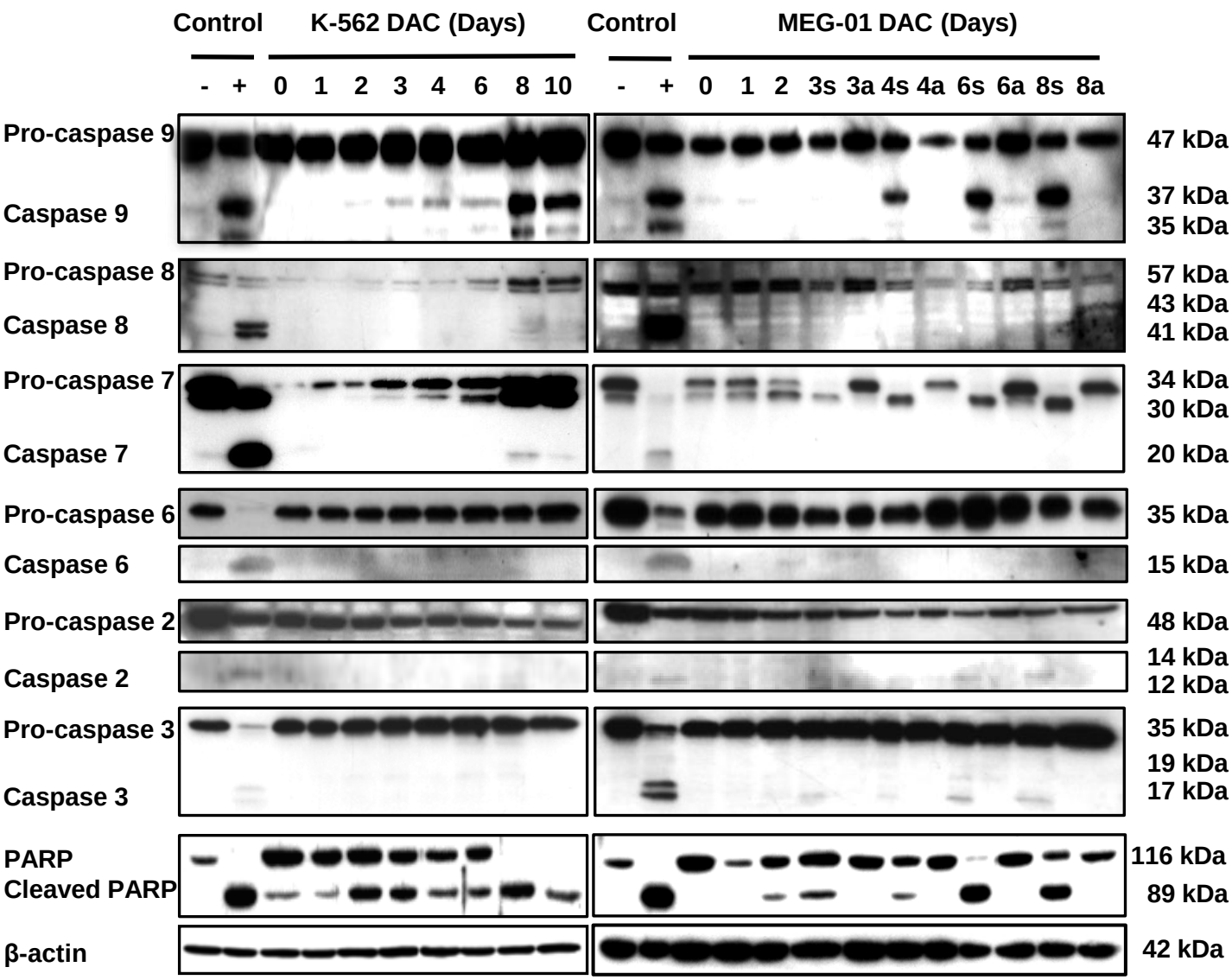
Control
K-562 DAC (Days)
Control
MEG-01 DAC (Days)
- + 0 1 2 3 4 6 8 10
- + 0 1 2 3s 3a 4s 4a 6s 6a 8s 8a
Pro-caspase 9
Caspase 9
47 kDa
37 kDa
35 kDa
Pro-caspase 8
Caspase 8
57 kDa
43 kDa
41 kDa
Pro-caspase 7
Caspase 7
34 kDa
30 kDa
20 kDa
Pro-caspase 6
Caspase 6
35 kDa
15 kDa
Pro-caspase 2
Caspase 2
48 kDa
14 kDa
12 kDa
Pro-caspase 3
Caspase 3
35 kDa
19 kDa
17 kDa
PARP
Cleaved PARP
116 kDa
89 kDa
β-actin
42 kDa

E

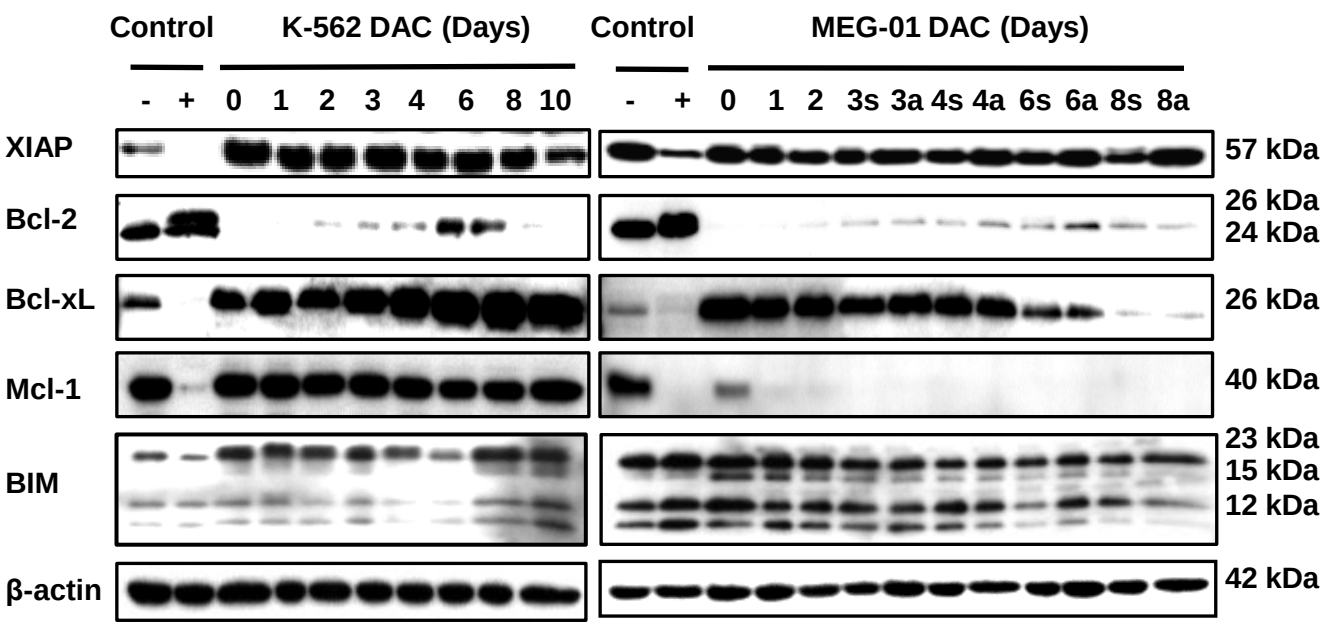
Control
K-562 DAC (Days)
Control
MEG-01 DAC (Days)
- + 0 1 2 3 4 6 8 10
- + 0 1 2 3s 3a 4s 4a 6s 6a 8s 8a
XIAP
57 kDa
Bcl-2
26 kDa
24 kDa
Bcl-xL
26 kDa
Mcl-1
40 kDa
BIM
23 kDa
15 kDa
12 kDa
β-actin
42 kDa

A

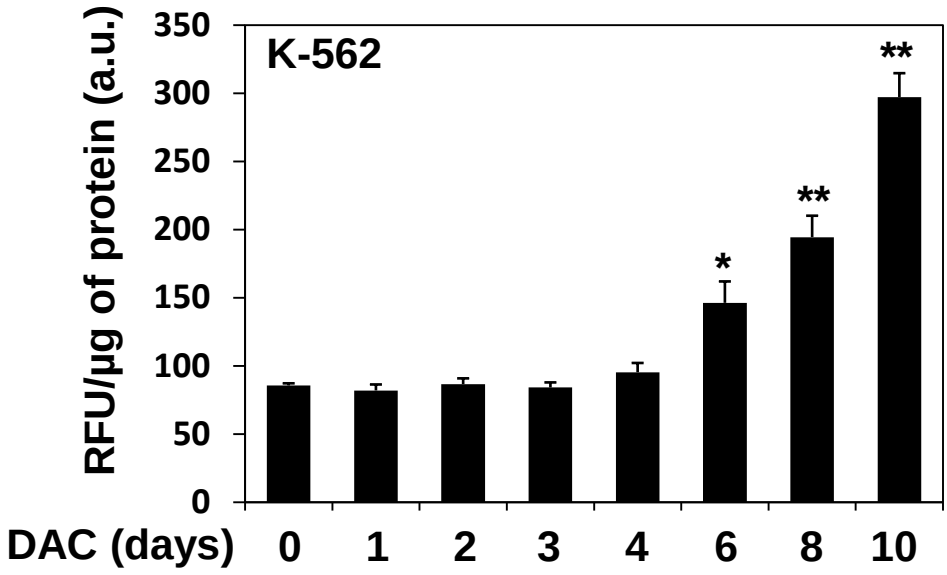
K-562
RFU/µg of protein (a.u.)
350
300
250
200
150
100
50
0
DAC (days)
0
1
2
3
4
6
8
10
*
**
**
**

B

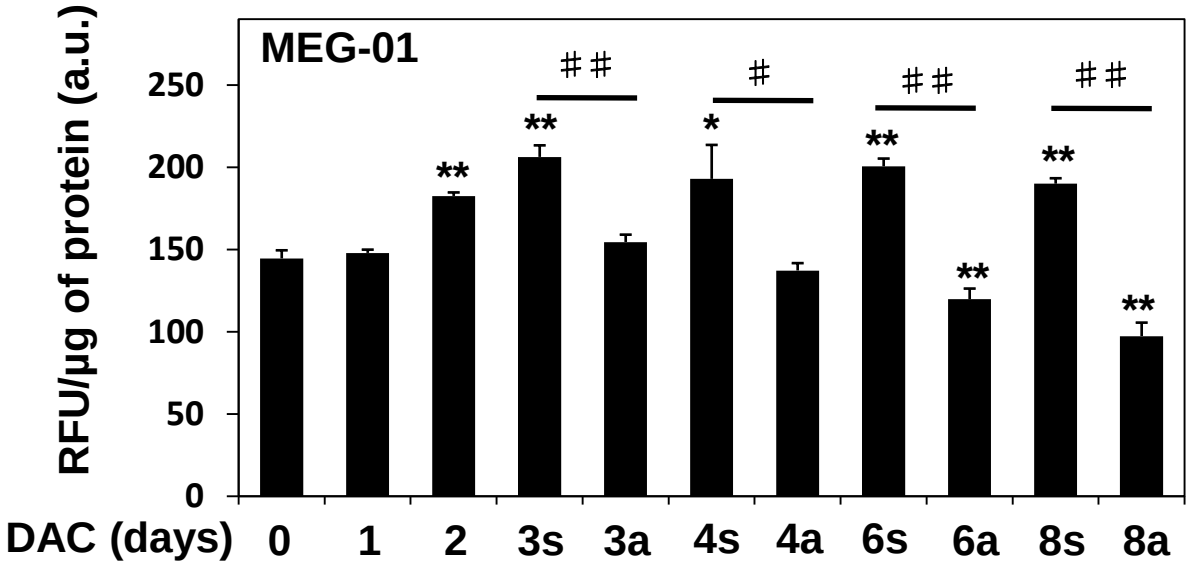
MEG-01
RFU/µg of protein (a.u.)
250
200
150
100
50
0
DAC (days)
0
1
2
3s
3a
4s
4a
6s
6a
8s
8a
**
**
*
**
**
**
**
**
##
#
##
##

A

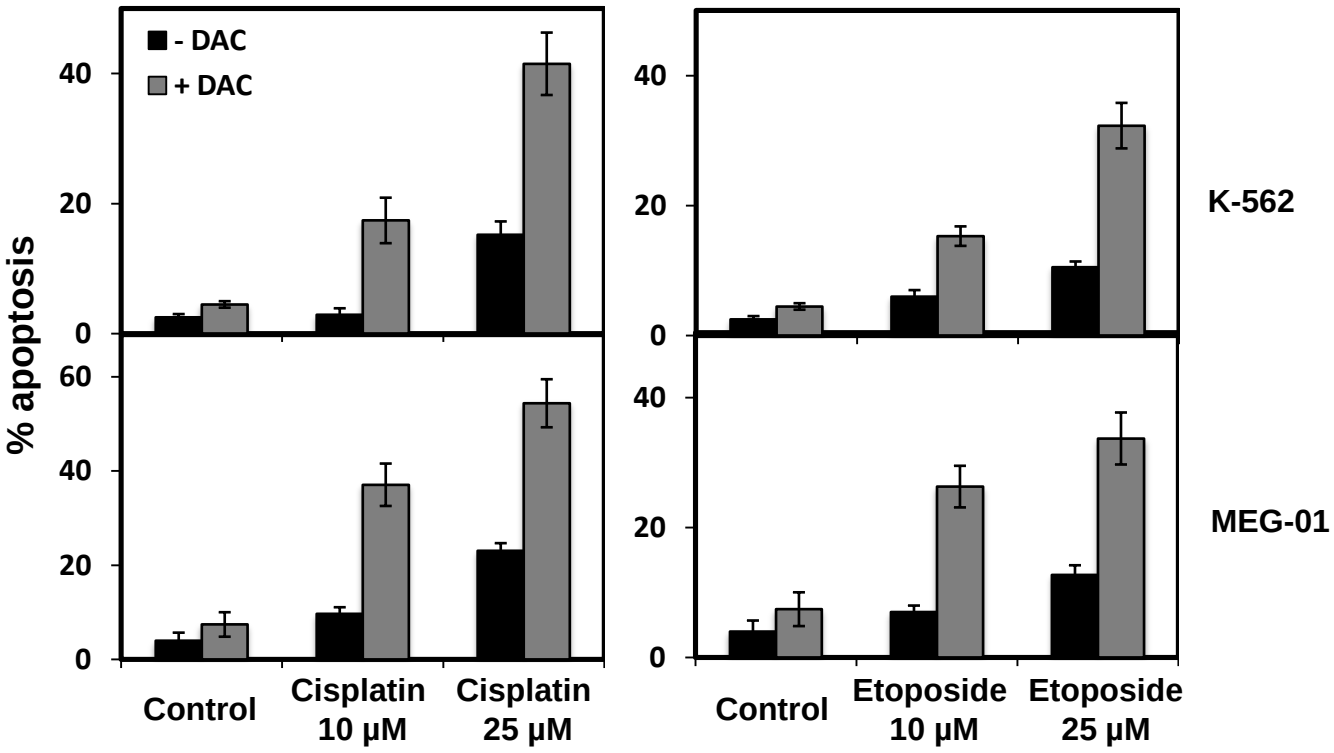
- DAC
+ DAC
% apoptosis
K-562
MEG-01
Control
Cisplatin 10 μM
Cisplatin 25 μM
Control
Etoposide 10 μM
Etoposide 25 μM

B

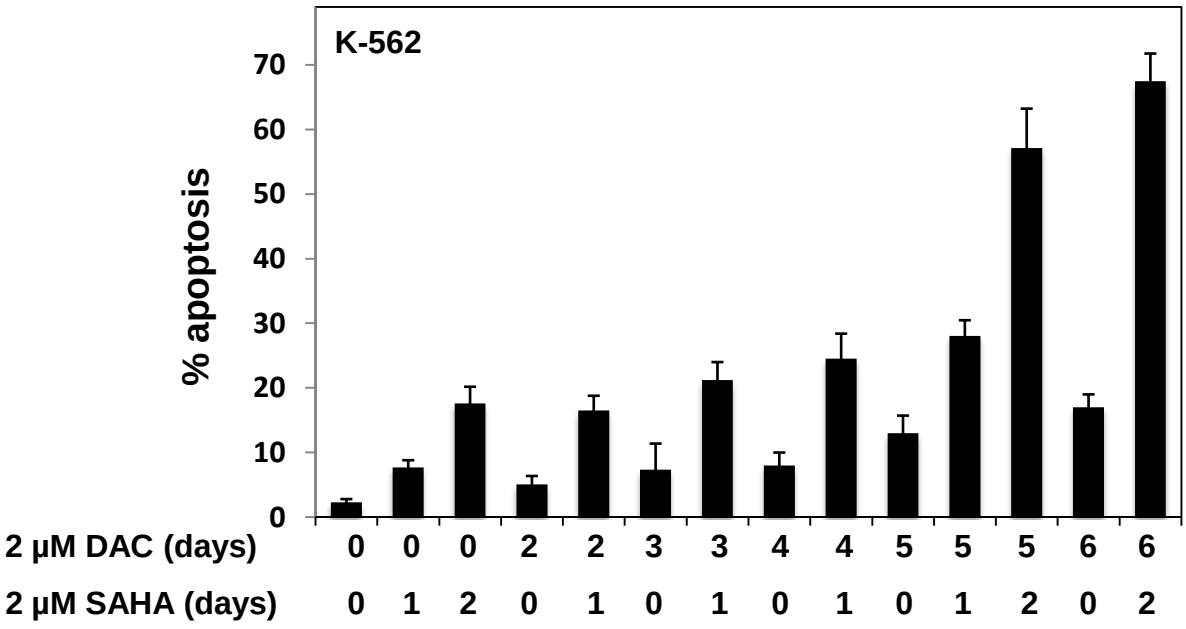
K-562
% apoptosis
2 μM DAC (days) 0 0 0 2 2 3 3 4 4 5 5 5 6 6
2 μM SAHA (days) 0 1 2 0 1 0 1 0 1 0 1 2 0 2

C

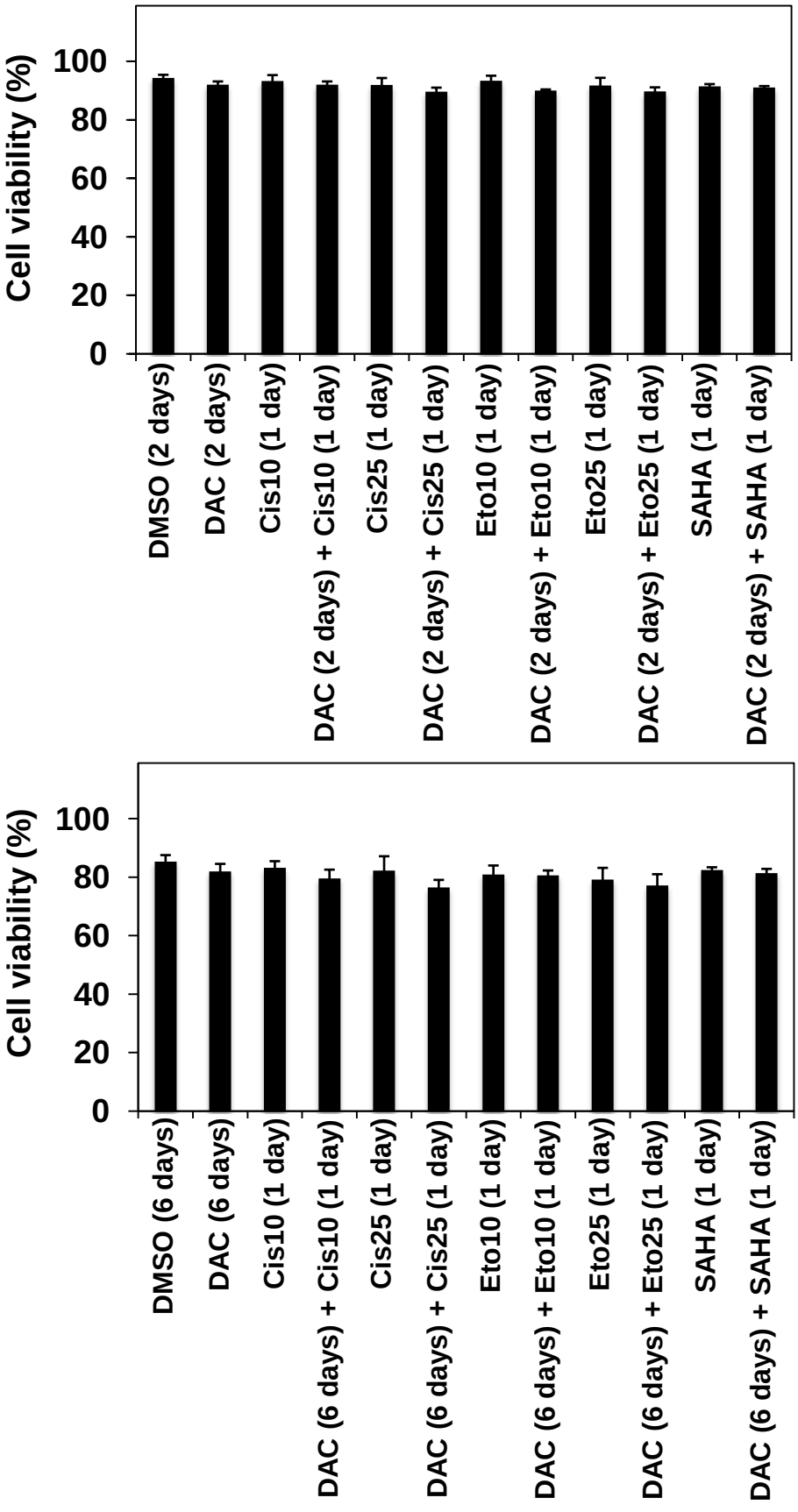
Cell viability (%)
0
20
40
60
80
100
DMSO (2 days)
DAC (2 days)
Cis10 (1 day)
DAC (2 days) + Cis10 (1 day)
Cis25 (1 day)
DAC (2 days) + Cis25 (1 day)
Eto10 (1 day)
DAC (2 days) + Eto10 (1 day)
Eto25 (1 day)
DAC (2 days) + Eto25 (1 day)
SAHA (1 day)
DAC (2 days) + SAHA (1 day)
Cell viability (%)
0
20
40
60
80
100
DMSO (6 days)
DAC (6 days)
Cis10 (1 day)
DAC (6 days) + Cis10 (1 day)
Cis25 (1 day)
DAC (6 days) + Cis25 (1 day)
Eto10 (1 day)
DAC (6 days) + Eto10 (1 day)
Eto25 (1 day)
DAC (6 days) + Eto25 (1 day)
SAHA (1 day)
DAC (6 days) + SAHA (1 day)